Second of 1
1 Copies
P
033548

NASA TECHNICAL NOTE

NASA TN D-2945

NASA TN D-2945

AD-A TIAC

DISTRIBUTION STATEMENT A
Approved for Public Release
Distribution Unlimited

BLAST EFFECTS ON SPACE VEHICLE STRUCTURES

by Reino Niemi and Richard Rabenau

George C. Marshall Space Flight Center
Huntsville, Ala.

20020320 227

NATIONAL AERONAUTICS AND SPACE ADMINISTRATION • WASHINGTON, D. C. • FEBRUARY 1966

NASA TN D-2945

BLAST EFFECTS ON SPACE VEHICLE STRUCTURES

By Reino Niemi and Richard Rabenau

George C. Marshall Space Flight Center
Huntsville, Ala.

NATIONAL AERONAUTICS AND SPACE ADMINISTRATION

For sale by the Clearinghouse for Federal Scientific and Technical Information
Springfield, Virginia 22151 – Price $3.00

TABLE OF CONTENTS

LIST OF ILLUSTRATIONS

LIST OF ILLUSTRATIONS (Cont'd)

LIST OF ILLUSTRATIONS (Cont'd)

LIST OF TABLES

CONVERSION TABLE TO THE INTERNATIONAL SYSTEM OF UNITS

To convert from...	to...	Multiply by...
ton	kilogram	907.18
pound	kilogram	.45359
inch	meter	.0254
foot	meter	.3048
yard	meter	.9144
$lbm/foot^3$	$kilogram/meter^3$	16.018
$inch^2$	$meter^2$	.00064516
foot/second	meter/second	.3048
psi ($lbf/inch^2$)	$newton/meter^2$	6894.7

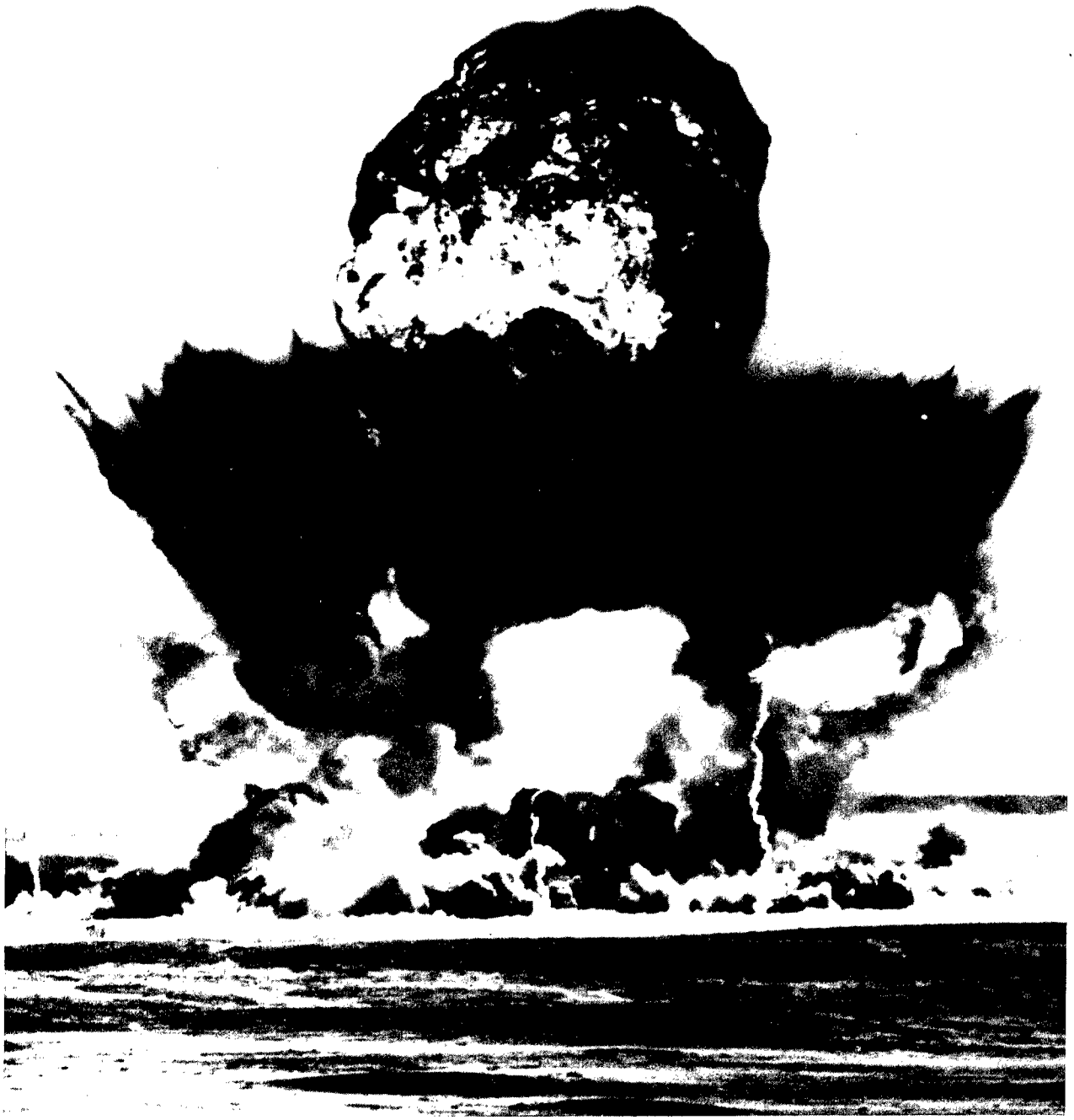

THE 500 TON DETONATION

BLAST EFFECTS ON SPACE VEHICLE STRUCTURES

SUMMARY

The purpose of participating in the explosive test was to obtain blast overpressure data, structural response data and to evaluate effectiveness of typical flight instrumentation for measuring blast effects.

Data were obtained on pressure loading of a structure as well as response of the structure to the loading.

The different types of gages utilized in the test were strain gages, piezoelectric microphones, strain gage pressure transducers and piezoelectric accelerometers. All gages except the strain gage pressure transducers were partially or wholly effective in measuring blast and structural response parameters.

INTRODUCTION

NASA participated in the 500 Ton High Explosive Detonation Test, Operation Snowball, conducted at Suffield Experimental Station, Alberta, Canada, in July 1964. United States participation was under the technical and administrative supervision of the Defense Atomic Support Agency.

NASA is currently developing and testing large liquid propellent space vehicle configurations under the Saturn program. The liquid oxygen, liquid hydrogen and RP-1 (kerosene) used as fuel in the booster and upper stages, could, in the event of catastrophic failure, produce an explosion equivalent to many tons of TNT. Saturn vehicles are designed to withstand a specified blast overpressure while in launch configuration. Saturn V Design Ground Rules require the booster, in launch configuration, to be able to withstand a 0.4 psi peak blast overpressure.

In order to experimentally verify these design requirements, the environment must be simulated as closely as possible. That is, the peak overpressure and positive duration must be close to predicted values for a catastrophic failure. The test specimen must be typical of the entire structure and the terrain must be similar to the launch area. The 500 Ton High Explosive Detonation Test was an excellent opportunity to evaluate the design criteria for a blast environment.

The experiment was conducted at the Watching Hill Blasting Range, Suffield Experimental Station (see Fig. 1). The site is a dry lake bed, very flat with little vegetation. A 0.5 psi peak overpressure was selected as the test level since it slightly exceeds ground rule requirements. The test specimen was located 7500 feet from ground zero corresponding to the 0.5 psi overpressure. This distance was extrapolated on the graph in Figure 2. This graph was based on information obtained from the 100 Ton Test in 1961 and previous smaller tests. The distance was also verified from information in Reference 1. A cylindrical section of Saturn I LOX tank was selected as the test specimen. This section of tank was identical to a flight tank and representative of the entire structure. The test environment is described in Table I. The structural details are listed in Table II and views of the cylinder are shown in Figures 3 and 4.

OBJECTIVES

The overall objective of the project was to acquire data on the response of typical space vehicle structure to a blast environment. Data were required which would aid in validating the overpressure requirements established in Saturn V Design Ground Rules Document, as explained previously.

A secondary objective of the project was to evaluate the effectiveness of typical flight instrumentation in determining structural response to a blast environment. Because the instrumentation available on a launch vehicle consists of accelerometers, strain gages, and microphones, these transducers would provide data to evaluate structural response and integrity in the event of an adjacent catastrophic failure.

THEORY

A detonation quickly releases a large amount of energy. A large portion of this energy travels outward in all directions from the point of detonation in the form of a spherical high pressure wave. In this report, the leading edge of this high pressure wave is called the shock front. The shock front propagates outward from the detonation point at a velocity greater than the speed of sound and gradually decreases with distance to the ambient sound velocity. The shock front incident pressure, called the blast overpressure, also decreases rapidly as it travels away from the source. Shock front positive and negative pressure phases

are of primary importance due to their high energy content. Another effect of the blast wave, the dynamic pressure, is an important effect at short ranges, but becomes negligible at long ranges.

The shock front, immediately after detonation, has a sharp leading edge and the positive overpressure has a very short time period. As the front propagates outward, the pressure amplitude decreases and the positive overpressure time period increases. Thus, at relatively great distances from the detonation, the blast wave energy is contained in a narrow low frequency spectrum. Previous test results indicate that the frequency spectrum below 100 cycles per second contains most of the energy. [2]*

The method described in the following text was used to calculate pressure variation and structural loading values. These values were used to establish calibration ranges of microphones and pressure pickups.

The blast wave variation at the specific test location chosen is depicted by Figure 5 . This pressure history will be seen by a point on the tank as the wave passes. The general situation for pressure variation around a cylinder is shown in Figure 6 . In this figure y represents any point on the surface.

The reflected pressure varies with the position of y and the angle β . The reflected pressure as a function of β may be seen in Figure 7 . The reflected pressure builds up on the front of the obstruction and is the load seen by that obstruction. In Figure (7), P is the incident overpressure and P_r is the reflected overpressure at any arbitrary point.

The decay time, t_d, is given by $\frac{3r}{U}$ which is equal to 7.7 msec. at $\beta = 0$ degree and decreases linearly to 0 at $\beta = 90$ degrees as shown in Figure 8 . At any time, t, the pressure is given by the expression $p_t = p(t + \frac{x}{U})$. Figure 9 shows the pressure normal to the surface at any point y.

Figure 10 shows the rise time, t_r, on the back half of the cylinder. The rise time increases linearly as β increases from 90 degrees through 180 degrees and reaches a maximum of 5.13 msec. at $\beta = 180$ degrees.

Figure 11 shows the pressure normal to the surface at any point on the cylinder, $\beta = 90$ degrees to $\beta = 180$ degrees.

---

* Numerals in brackets denote reference.

Based on the selection of 0.5 psi as the desired overpressure, the blast wave characteristics were calculated as follows: the ambient conditions listed below were utilized in the calculations [3]. The elevation of the test area is 2168 feet [4].

p_0 (ambient pressure) = 13.8 psi
c_0 (ambient sound velocity) = 1025 ft/s
ρ_0 (ambient density) = 0.0692 lb/ft^3

This distance from ground zero for a 0.5 psi peak overpressure is 7500 feet as read on Figure 12 and extrapolated on Figure 13 [5]. The positive overpressure duration is 480 milliseconds [5].

The shock velocity, U, is:[1]

$$U = c_o \left[1 + \frac{6\,p}{7\,P_o}\right]^{1/2} = 1025 \left[1 + \frac{6\,(0.5)}{7\,(13.8)}\right]^{1/2}$$

$$= 1025\,(1 + 0.031)^{1/2}$$

$$U = 1040 \text{ ft/s.}$$

The particle velocity, U, behind the shock front is:[1]

$$U = \frac{5\,p}{7\,p_o}\left[\frac{c_o}{(1 + \frac{6\,p}{7\,p_o})^{1/2}}\right] = \frac{5\,(0.5)}{7\,(13.8)}\left[\frac{341}{1.015}\right]$$

$$= 8.71 \text{ ft/sec .}$$

The density, ρ, of the air behind the shock front is: [1]

$$\frac{\rho}{\rho_o} = \left[\frac{7 + \frac{6\,p}{p_o}}{7 + \frac{p}{p_o}}\right] p_o \text{ ,}$$

$$\rho = 0.692 \left[\frac{7 + \frac{6\ (0.5)}{13.8}}{7 + \frac{0.5}{13.8}} \right]$$

$$\rho = 0.712 \text{ lb/ft}^3 .$$

The dynamic pressure, q, is: [1]

$$q = \frac{5}{2} \left[\frac{p^2}{7\ p_o + p} \right] = \frac{5}{2} \left[\frac{(0.5)^2}{7\ (13.8) + 0.5} \right] ,$$

q = .0065 psi as extrapolated on Figure 14.

The duration of the positive impulse was ascertained on Figure 15.

The reflected pressure generated on the front of an obstacle (in this case the cylinder) is: [6]

$$p_r = 2p \left[\frac{7\ p_o + 4\ p}{7\ p_o + p} \right] ,$$

$$= 2\ (0.5) \left[\frac{7\ (13.8) + 4\ (0.5)}{7\ (13.8) + 0.5} \right] ,$$

$$= 1.01 \text{ psi} .$$

The amplitude of the ground shock, A, is: [6]

$$A = \frac{C^{2/3}}{100} \left[0.07\ e^{-0.00143\ d} + 0.001 \right] ,$$

where C = weight of charge in lbs
d = distance in feet
A = displacement of ground [1]

Some of the characteristics of the blast wave were not calculated but were obtained from technical literature.

Frequencies in ground shock : 1/2 to 100 cps [2]
Peak negative pressure: 0.15 psi [1]
Peak negative pressure duration: 0.8 seconds [1]

Based on the above pressure calculations, a summary of the anticipated overpressure effects at the cylinder location are presented:

When the pressure front of 0.5 psi envelops the front of the cylinder, the obstruction to flow will cause the pressure on the forward side of the cylinder to rise to a value near the calculated reflected pressure of 1.0 psi. The reflected pressure will quickly decay to the value of the incident overpressure, 0.5 psi. The reflected pressure will decrease approximately linearly from a maximum of 1.0 psi on the tank forward side to a value of 0.5 psi on the side of the cylinder. As the incident pressure engulfs the cylinder, the pressure on the rear side of the tank will take a finite time to rise to the full value of the incident overpressure. Following the positive phase of the incident overpressure, the pressure will drop to an estimated value of 0.15 psi below ambient pressure. The pressure then will rise quickly to the ambient condition. No further significant effects of the blast wave will be present at this location.

The preliminary calculations of blast response accelerations were made to establish the appropriate calibration range for the instrumentation system. The precedure used was based upon empirically derived equations and data generated under NASA Contract NAS8-11514, "Experimental Determination of System Parameters for Thin-Walled Cylinders." These equations and data are presented in monthly and quarterly progress reports and in the "First Annual Summary Report," Republic Aviation report RAC 1117-6, June 29, 1964.

The method of response predictions involved predictions of the fundamental (lowest frequency) modes of shell response and an effective stiffness of the shell. The shell and its attached accelerometer and mounting block were analytically treated as a one-degree-of-freedom spring mass system. The blast pressure was considered to be an impulsive load distributed over one half wave (circumferential and longitudinal) of the response mode with a triangular pulse shape. The response displacement amplitude was calculated from the dynamic

load factor, the effective stiffness, and the effective pressure loading. This displacement was considered to be the peak displacement of the fundamental free vibration mode, and the associated acceleration was calculated assuming sinusoidal motion.

The above procedure has inherent errors because of the assumptions made, but it was felt to be sufficiently accurate for establishing calibration ranges. The Appendix gives the detailed calculations which were made in this problem.

To verify the calculated calibration ranges, small charges (17.5 lbs of TNT) were used to excite the tank. Together with the calculated values, results from the test were used to set ranges for vibration instrumentation. These tests also showed that the microphones would react linearly to shock front overpressure.

TEST PLAN

The basic test plan consisted of placing the section of LOX tank in the desired overpressure region and securely anchoring the base in concrete pilings. The tank was instrumented to measure circumferential pressure variation and dynamic response, as well as seismic shock. In addition, pressure measurements were made on a blast radius to determine free field shock characteristics near the tank. Recording instrumentation was located in an instrumentation trailer parked 1200 feet beyond the tank at 8700 feet from ground zero. The trailer was manned in a calculated 0.41 psi, 150 db overpressure area, situated head-on to the blast. No provisions were made to protect the trailer from the overpressure condition. The overall test setup, including the dome shaped building which housed the charge is shown in Figure 16 . A description of the charge is presented in Table III.

INSTRUMENTATION

Seven microphones were flush mounted on the cylinder at 30-degree intervals as shown in Figure 17 , to measure the pressure distribution. A block diagram of the measuring system is shown in Figure 18 . The system included a vibration compensating flight type piezoelectric microphone, a field signal conditioning unit to condition the signal for transmission on a balanced pair of unshielded lines (infantry communications field wire type wd-1/tt),

a line receiving unit which terminated the balanced lines in the trailer, and isolation amplifier and a tape recorder. The system signal-to-noise ratio was 34 db. The system was slightly underdamped. For the length of line utilized in this system, the response was within ±2 db from 1 cycle per second to 10 kilocycles per second, excluding the microphone. The tape recorders were 14-track FM having a frequency response of DC to 20 kilocycles per second. Figure 19 shows a typical microphone and accelerometer installation.

Three flight type strain gage pressure transducers were mounted at 90-degree intervals on the tank circumference, as shown in Figure 17 , to supplement other pressure distribution measurements. The gages had DC to 600 cycle per second response and the system dynamic range was 34 db. The data acquisition system used with the strain gage pressure transducers was a multi-channel Wheatstone bridge carrier system terminated at a recorder. A common 3 kilocycle per second oscillator provided a carrier signal for all channels. A block diagram of the system is shown in Figure 20 .

Five shock mounted piezoelectric microphones were placed at 100-foot intervals on a radius of the blast, as shown in Figure 21 , to measure the free field pressure. The data transmission system was the same as that utilized for pressure measurements on the cylinder.

Six piezoelectric accelerometers were mounted on the circumference of the cylinder to measure the shock impulse. Three gages were at 90-degree intervals on the open panel; three at 90-degree intervals on the upper ring stiffener. The gages had a frequency response of 3 cycles per second to 10 kilocycles per second. One accelerometer was mounted on a rigid section on the top of the tank to measure overall cylinder response. This gage had a frequency response of 2 cycles per second to 4 kilocycles per second. These measurements are shown in Figure 17 . The system used to transmit these measurements was the same as that utilized for the microphones.

In addition to the crystal accelerometer, twelve strain gages were used to measure strain in the vertical and horizontal planes and overall bending as shown in Figure 17 . The data transmission system was the same as that utilized for the strain gage pressure transducers.

A piezoelectric accelerometer was mounted normal to the surface of the earth on the cylinder base framework as shown in Figure 17 . The gage was of very high sensitivity, generating a voltage of 300 millivolts per G excitation. It had a frequency response of 2 cycles per second to 2.5 kilocycles per second. A bending mode accelerometer with a response of approximately 5 cycles per second to 20 cycles per second was used to measure the seismic effect on the top of the cylinder in a plane normal to a blast radius (see Fig. 17). The system used for this measurement was the same as that utilized for the microphones.

DATA

Some of the pressure measurement microphone channels on the test cylinder (Fig. 17) did not function properly. However, enough did function to furnish overpressure data on the structure and to indicate the suitability of microphones for low overpressure measurements. The microphone on the leading edge of the cylinder recorded a peak overpressure level of 1.06 psi. (Fig. 22, Measurement No. 1)[1]. This was greater than the incident overpressure level and showed the predicted overpressure level due to reflection. The reflected overpressure duration was close to the predicted value (7.7 msec). The measured time from detonation for the shock front to reach the cylinder was 5.1 seconds which was near the predicted arrival time read on Figure 24.

The next microphone around the cylinder at 30 degrees from the leading edge did not respond, which probably indicated instrumentation failure. The microphone was found to be in satisfactory condition following the test, which indicates signal conditioning or recording equipment failure. The microphone at 60 degrees from the leading edge recorded a level of 0.94 psi (Fig. 25, Measurement No. 3). This again showed the effect of reflected overpressure. The reflected overpressure duration was close to the predicted value. The lag time for the pressure front to reach this point was 1285 microseconds referenced to pressure Measurement Number 1 on the leading edge of the cylinder. The microphone at 90 degrees from the leading edge recorded a level of 0.50 psi overpressure. (Fig. 26 and 27, Measurement No. 4). This reading indicated the level of incident overpressure as predicted.

The lag time referenced to Measurement Number 1 was 2570 microseconds. The microphone at 120 degrees did not operate. The microphone at 150 degrees from the leading edge recorded a level of 0.4 (Fig. 28, Measurement No. 6). This measurement took 3.6 milliseconds to rise to maximum value (see Fig. 10 and 11 for predicted values). The lag time referenced to Measurement Number 1 was 4795 microseconds. The measurement at 180 degrees did not respond. The durations of the positive overpressures were much less than anticipated. (See Fig. 29 for predicted values.) These short durations cannot be considered valid since close examination of the data indicated that the transient nature of the pressure input caused a damped low frequency oscillation in the measuring circuits. Also low frequency roll-off of the measuring system affected the overpressure duration values. It should be noted here that data obtained from other sources indicated that the positive overpressure duration was close to the predicted value of 480 milliseconds and that the incident overpressure level was 0.5 psi.

[1] Acoustic Calibrations were made in db using 0.0002 dynes/cm^2 as reference. This db value is in terms of RMS, not peak, since the reference pressure is in RMS. The measured data were then converted to psi (RMS) by means of the conversion table (Fig. 23) and multiplied by 1.4 to convert to peak pressure. The values shown on the raw data are in terms of peak values. Table IV gives acoustic calibrations in terms of psi peak also.

Measurements 32 through 36 were shock mounted microphones used as pressure sensors on a blast radius (Fig. 21). Measurement 32 read 0.5 psi (Fig. 30), Measurement 33 read 0.53 psi (Fig. 31), Measurement 34 read 0.60 psi, Measurement 35 read 0.66 psi (Fig. 32), and Measurement 36 read 0.42 psi. These measurements indicated a damped low frequency oscillation induced in the system and thus invalidated the pressure duration information.

Measurements 14, 15 and 16 were strain gage pressure tranducers located at 0, 90 and 180 degrees respectively, on the cylinder ring stiffener (Fig. 17). The resonant frequency of these instruments was excited by the pressure front and valid data were not obtained from these gages. These gages were thus considered unsatisfactory for measurement of shock wave pressure.

Accelerometer Measurements 30 and 31 were used to define the cantilever bending of the cylinder (Fig. 17), with Measurement 30 (Fig. 33) recording a maximum G level of 7.0 G's zero to peak while Measurement 31 (Fig. 34) read 5.5 G's zero to peak. Measurement 30 was sensitive in a plane parallel to the blast radius and Measurement 31 measured in a plan normal to the blast radius.

Measurements 8 (Fig. 35), 9 (Fig. 36) and 10 (Fig. 37), were located at 0, 90 and 180 degrees respectively on the cylinder ring stiffener (Fig. 17). These measurements read 90 G's 43 G's and 40 G's, zero to peak, respectively. Measurement Number 8 was biased due to an FM record amplifier. However, since the data were symmetrical about the mean, no information was lost.

Measurements 11, 12 (Fig. 38) and 13 (Fig. 39) were located at 0, 90 and 180 degrees on unbraced skin panel (Fig. 17). Measurement 11 did not record. The other two recorded levels of 42 G's, zero to peak and 20 G's, zero to peak, respectively.

Measurement 29 (Fig. 40 and 41) recorded a vertical movement of 1.5 G's zero to peak for the overall structure when the shock wave arrived (Fig. 17). This accelerometer was to have recorded the seismic acceleration but the level was lower than predicted and was not measured. Measurement Number 37 recorded a vertical acceleration of 0.2 G's zero to peak as the ground shock passed and 1.8 G's zero to peak as the air shock wave passed the cylinder (see Fig. 42 and 43).

The stress levels obtained varied over a wide range. Indications are that most of the data obtained was invalid. Many problems were encountered in checking out the strain gage instrumentation in the field, mainly due to the long cable runs. Also, the range at which the strain gage circuits were calibrated, 120 microinches/inch, was very sensitive and made setup very different. The

effects of wind and temperature were noticeable on the gages. The anticipated stress levels were 50 microinches/inch. Some of the gage readings (five) were close to the predicted level. However, the results were considered inconclusive for purposes of this report and are not presented.

CONCLUSIONS

The High Explosive Detonation Test proved that the Saturn rocket structure could withstand the blast overpressure as set forth in the Design Ground Rules. The experimental data obtained was satisfactory for evaluating the structural response. According to the data the structure underwent no detrimental effects from the blast overpressure. The predicted levels corresponded accurately to the experimental ranges of response.

The Saturn flight type instrumentation utilized for the test, with the exception of the strain gage pressure transducers, was partially or wholly effective in obtaining blast overpressure and structural response data. Therefore, these flight type instruments can be used as an indication of structural loading on a space vehicle resulting from an adjacent catastrophic failure. Of course not all gages would provide useful information because of the calibration ranges.

The flight type microphones would furnish useful initial pressure amplitude information, but the telemetry system bandpass (50 - 3000 cps) would not allow passage of pressure duration information. However, it should be noted that if the initial amplitude is accurately measured and the distance from the charge is known, other information such as overpressure duration can be calculated quite accurately.

The piezoelectric accelerometers worked very successfully in measuring shock impulse effect on the cylinder. The data obtained were well within the frequency range of standard piezoelectric accelerometers.

George C. Marshall Space Flight Center,
National Aeronautics and Space Administration,
Huntsville, Alabama, May 12, 1965

APPENDIX

PROCEDURE FOR APPROXIMATE CALCULATION OF BLAST RESPONSE ACCELERATION*

Problem Statement

The problem is to find the approximate response acceleration of a cylindrical shell structure with reinforced rings to a blast overpressure.

Method of Solution

The blast overpressure was considered to be an empirical load applied to the shell. The shell was considered to respond as a one-degree-of-freedom system at its lowest frequency mode of free vibration. The mode and frequency of the shell were determined from empirical methods developed by Republic Aviation, and the effective mass and stiffness of the mass spring analog were established from the same work [7]. The magnitude of the impulsive load was determined from an "effective area" determined by the mode shape, the speed of the blast shock front, and shell geometry. Response displacement, X, was calculated from the equation

$$X = (D.L.F.)\ (\ p\ )\ (\ \bar{A}\ )\ (\ \bar{K}\ )^{-1}$$

where

D. L. F. = dynamic load factor

p = blast overpressure

$\bar{A}$ = effective loading area on the shell

$\bar{K}$ = effective stiffness of the shell

Response acceleration was calculated from the sinusoidal motions relation

$$G = 0.102\ (f)^2\ (X)$$

where

* This procedure is based on Reference 7. In the discussion, Reference 7 is referred to as "the Reference" or is designated by a numeral in brackets, i.e., [7].

G = acceleration in earth gravities

f = frequency in cycles per second

Calculations

The pertinent specimen characteristics, in terms of the Reference are:

a = radius = 35 inches

L = ring spacing = 30 inches

h = skin thickness = 0.090 inch

E = Young's Modulus = 10^7 psi

p = Material sensitivity = 0.10 lb/in.^{3}

The geometric parameters (a/h, L/a) for this specimen agreed closely with cylinder 13a of the Reference program. The scale factor between the two was approximately 2:1; the frequencies obtained for specimen 13a would be roughly twice those expected for the blast experiment specimen. From the Reference it was noted that the fundamental mode for the subject specimen was one having 13 circumferential waves (26 half-waves) and one longitudinal half-wave between ring frames. This modal frequency was 270 cycles per second. Therefore, the same fundamental mode should occur in the blast test specimen at around 135 cycles per second.

The effective modal (point) stiffness of the shell was calculated from the empirical equation [7]

$$\bar{K} = (E\ a)\ (10)^{-6} \left[\bar{K}_1 + \bar{K}_2\left(\frac{P}{E}\right)\ (10^6) - \bar{K}_3\left(\frac{L}{a}\right)\right]$$

where $\bar{K}_1$, $\bar{K}_2$, and $\bar{K}_3$ are obtained from the Reference, and P is the internal pressure. Since there is no internal pressure, the $\bar{K}_2$ term is eliminated from the above equation. The value of $\bar{K}$ was found to be 910 pounds per inch for the blast specimen for a point on the shell half-way between two ring frames. This point corresponds to the location of measurements 11, 12, and 13 of the blast test.

A calculation of fundamental shell frequency was also made from the equation [7]

$$f = \frac{1}{2\pi} \left(\frac{386.4K}{W_e + W_a}\right)^{1/2} ,$$

where

W_e = effective cylinder weight

W_a = added (point) weight

The calculation of W_e is

$$W_e = \alpha_1 W_a + (a^2 ph)\ \alpha_2 \quad ,$$

where α_1 and α_2 are taken from the Reference and depend only on (a/h). The W_a was considered to be the added weight of an accelerometer and its mounting block which was 0.25 pounds. The calculated value of W_e is

$$W_e = (0.62)\ (0.25) + (35)^2\ (0.10)\ (0.090)\ (0.04)$$

$$W_e = 0.60 \text{ pounds} \quad .$$

The calculated value of fundamental frequency is

$$f = \frac{1}{6.28} \left(\frac{(386.4)(910)}{0.60 + 0.25} \right)^{1/2}$$

$$f = 102 \quad \text{cps}$$

This value agrees closely with that obtained for cylinder 13a of the Reference program, with the difference being partially explained by the effect of the added accelerometer and block mass.

At this point the one-degree-of-freedom analog of the local shell structure is defined as a mass of 0.85 pounds mounted on a spring of 910 pounds per inch stiffness with a fundamental frequency of 102 cycles per second. The next step was to determine the effective impulsive load imposed on this system and the resulting response acceleration.

The shock wave was expected to travel at approximately 1040 feet per second, or 12,480 inches per second. The projected distance from a point on the shell normal to the shock wave direction and the mode points of the half-wave for the fundamental mode described previously (26 circumferential half-waves) was found to be 0.30 inch. The time required for the shock wave to travel over one half-wave would therefore be:

$$T = \frac{0.30 \text{ inches}}{12,480 \text{ in/s}} = 24 \times 10^6 \text{ s} \quad ,$$

indicating that the entire half-mode surface can be considered as loaded simultaneously by the blast pressure.

The expected impulse load was simplified to a triangular pulse with a rise time of less than 1 millisecond and a decay time of 7 milliseconds with a peak pressure of 0.50 pounds per square inch. For this type loading, a dynamic load factor of 1.2 is considered to be conservative. Since the pressure is distributed over the entire half-wave surface, a mode shape factor is required in the displacement equation to account for the variations in effective stiffness over the surface. For sinusoidal mode shapes in two directions (longitudinal and circumferential) this mode shape factor is 0.25.

The effective displacement for the mass spring analog model under the impulsive loading is given by the equation

$$X = (D.L.F.)\ (p)\ (\bar{A})\,(\bar{K})^{-1},$$

where $\bar{A}$ is the effective loaded area including the mode shape factor (M.S.F.)

$$\bar{A} = (M.S.F.)(2\pi a)\ (\frac{1}{n})(L),$$

where n is the number of half waves.

$$\bar{A} = (0.25)(220)(\frac{1}{26})(30)$$

$$\bar{A} = 63.0 \text{ in.}^2 .$$

The effective peak displacement of the mass of the spring mass model is

$$X = (1.2)(0.5 \text{ psi})\ (63 \text{ in.}^2)(\frac{1 \text{ in.}}{910 \text{ lb.}})$$

$$X = 0.0415 \text{ in.} .$$

From the sinusoidal acceleration equation, the peak acceleration is

$$G = 0.102\ (f)^2(X)$$

$$G = 0.102\ (102)^2\,(0.0415)$$

$$G = 43$$

Conclusions

From these calculations it was concluded that the maximum response at a location midway between rings on the shell would be less than 50G. No calculation of ring accelerations was made, but they were estimated to be roughly one-half (or less) the accelerations calculated for the skin.

TABLE I. METEOROLOGICAL REPORT

Date:	July 17, 1964
Time:	10:58 MST
Site:	Watching Hill Blasting Range
	Temperature - 79° F at 2 ft.
	Wind Speed - 5 mph
	at 245° true azimuth
	Relative Humidity 41%
	Atmospheric Pressure 13.60 psi
	Conditions measured within 100 yards of tank, 7500 ft. from ground zero

TABLE II. TEST CYLINDER PARAMETERS

Diameter:	70 in
Height:	100 in
Weight:	450 lbs.
Skin Thickness:	.09 in
Material:	Aluminum alloy
Coefficient of drag:	.35
Max Projected Area:	7000 in^2
Pressurization:	None

TABLE III. DESCRIPTION OF EXPLOSIVE CHARGE

500 Ton Charge
The 500 Ton charge consisted of 30,800 cast TNT blocks each weighing 32.5 pounds and measuring 12 in X 12 in X 4 in. The individual blocks were stacked on a wooden base into a hemisphere with a 34 foot diameter. The charge contained a central tetryl booster for detonation.

TABLE IV. PROJECT 1.9 MEASUREMENT PROGRAM

MEAS No	TYPE MEAS	CALIBRATION LEVEL	MEASURED LEVEL	FREQUENCY RESPONSE	TYPE GAGE	MEASUREMENT DESCRIPTION, REFERENCE FROM GZ.
1	Pressure	1.29 psi	1.06 psi	1.0 cps to 10 K cps	Gulton P420M	Normal to Cylinder Skin, Flush Mount 360°
2	Pressure	1.29 psi	missed	1.0 cps to 10 K cps	Gulton P420M	Normal to Cylinder Skin, Flush Mount 330°
3	Pressure	0.73 psi	0.94 psi	1.0 cps to 10 K cps	Gulton P420M	Normal to Cylinder Skin, Flush Mount 300°
4	Pressure	0.73 psi	0.50 psi	1.0 cps to 10 K cps	Gulton P420M	Normal to Cylinder Skin, Flush Mount 270°
5	Pressure	0.73 psi	missed	1.0 cps to 10 K cps	Gulton P420M	Normal to Cylinder Skin, Flush Mount 240°
6	Pressure	0.73 psi	0.40 psi	1.0 cps to 10 K cps	Gulton P420M	Normal to Cylinder Skin, Flush Mount 210°
7	Pressure	0.73 psi	missed	1.0 cps to 10 K cps	Gulton P420M	Normal to Cylinder Skin, Flush Mount 180°
8	Vibration	± 30 g	90 g's	3 cps to 10 K cps	Cubit Corporation 2225	Normal to Skin at ring 360°
9	Vibration	± 30 g	43 g's	3 cps to 10 K cps	Cubit Corporation 2225	Normal to Skin at ring 270°
10	Vibration	± 30 g	40 g's	3 cps to 10 K cps	Cubit Corporation 2225	Normal to Skin at ring 180°
11	Vibration	± 40 g	missed	3 cps to 10 K cps	Cubit Corporation 2225	Normal to Skin unbraced 360°

TABLE IV. PROJECT 1.9 MEASUREMENT PROGRAM (CONCLUDED)

MEAS NO	TYPE MEAS	CALIBRATION LEVEL	MEASURED LEVEL	FREQUENCY RESPONSE	TYPE GAGE	MEASUREMENT DESCRIPTION, REFERENCE FROM GZ.	
12	Vibration	± 40 g	42 g's	3 cps to 10 K cps	Cubit Corporation 2225	Normal to Skin unbraced	270°
13	Vibration	± 40 g	20 g's	3 cps to 10 K cps	Cubit Corporation 2225	Normal to Skin unbraced	180°
29	Seismic	± 1 g	1.5 g's	2 cps to 2.5 K cps	Endevco 2619	Normal to Ground	360°
30	Vibration	± 30 g	7.0 g's	2 cps to 4 K cps	Endevco 2223C	Normal to Cylinder and Parallel to Blast Radius	360°
31	Vibration	± 10 g	5.5 g's	2 cps to 4 K cps	Endevco 2223C	Horizontal and Normal to Blast Radius	360°
32	Pressure	0.73 psi	0.50 psi	1.0 cps to 10 K cps	Chesapeake NM135	Parallel to Blast Radius at 7300 ft	
33	Pressure	0.73 psi	0.50 psi	1.0 cps to 10 K cps	Chesapeake NM135	Parallel to Blast Radius at 7400 ft	
34	Pressure	0.73 psi	0.60 psi	1.0 cps to 10 K cps	Chesapeake NM135	Parallel to Blast Radius at 7500 ft	
35	Pressure	0.73 psi	0.66 psi	1.0 cps to 10 K cps	Chesapeake NM135	Parallel to Blast Radius at 7600 ft	
36	Pressure	0.73 psi	0.42 psi	1.0 cps to 10 K cps	Chesapeake NM135	Parallel to Blast Radius at 7700 ft	
37	Vibration	± 1 g	1.8 g's	5 cps to 20 cps	Donner		

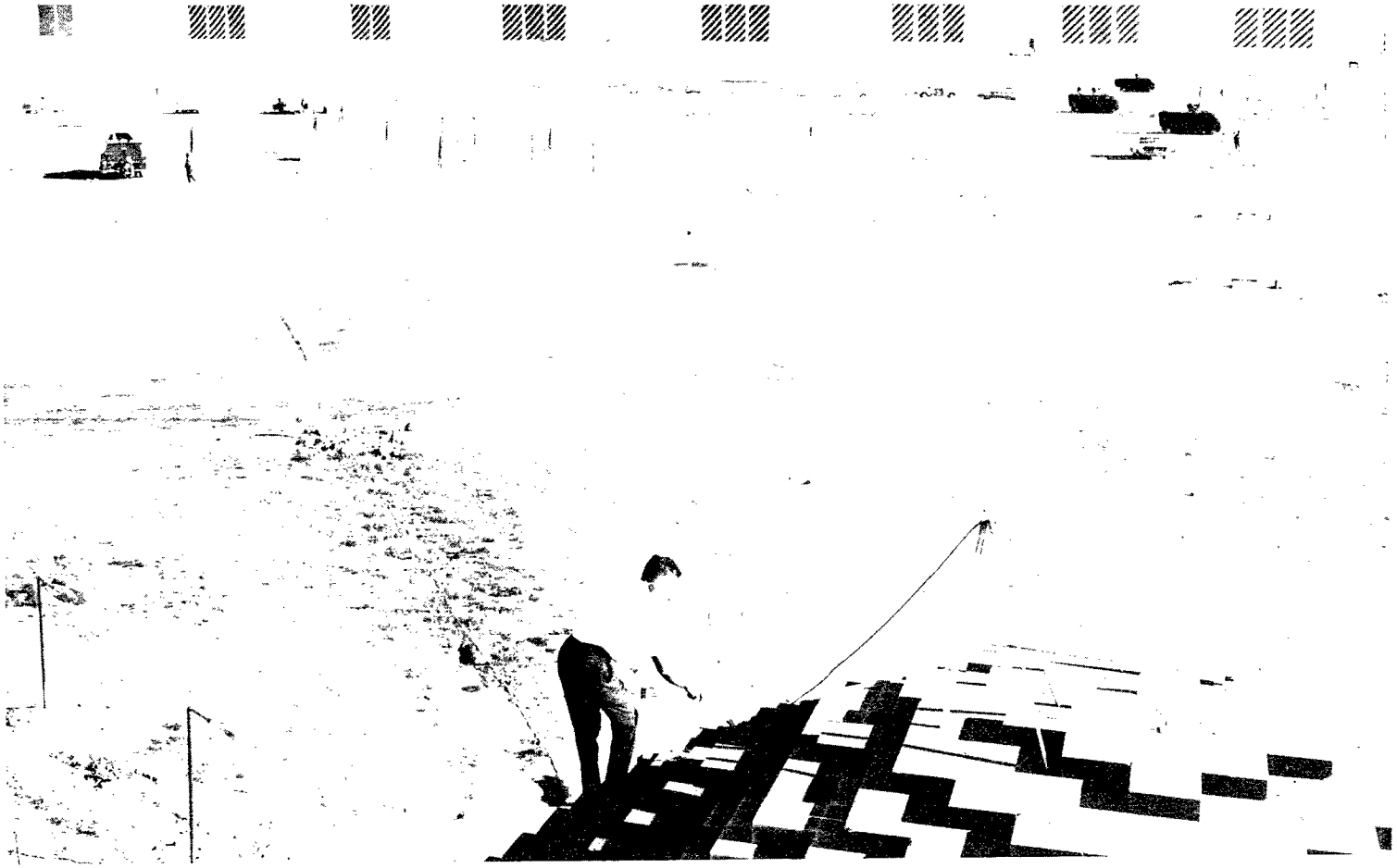

FIGURE 1. TEST SITE TERRAIN

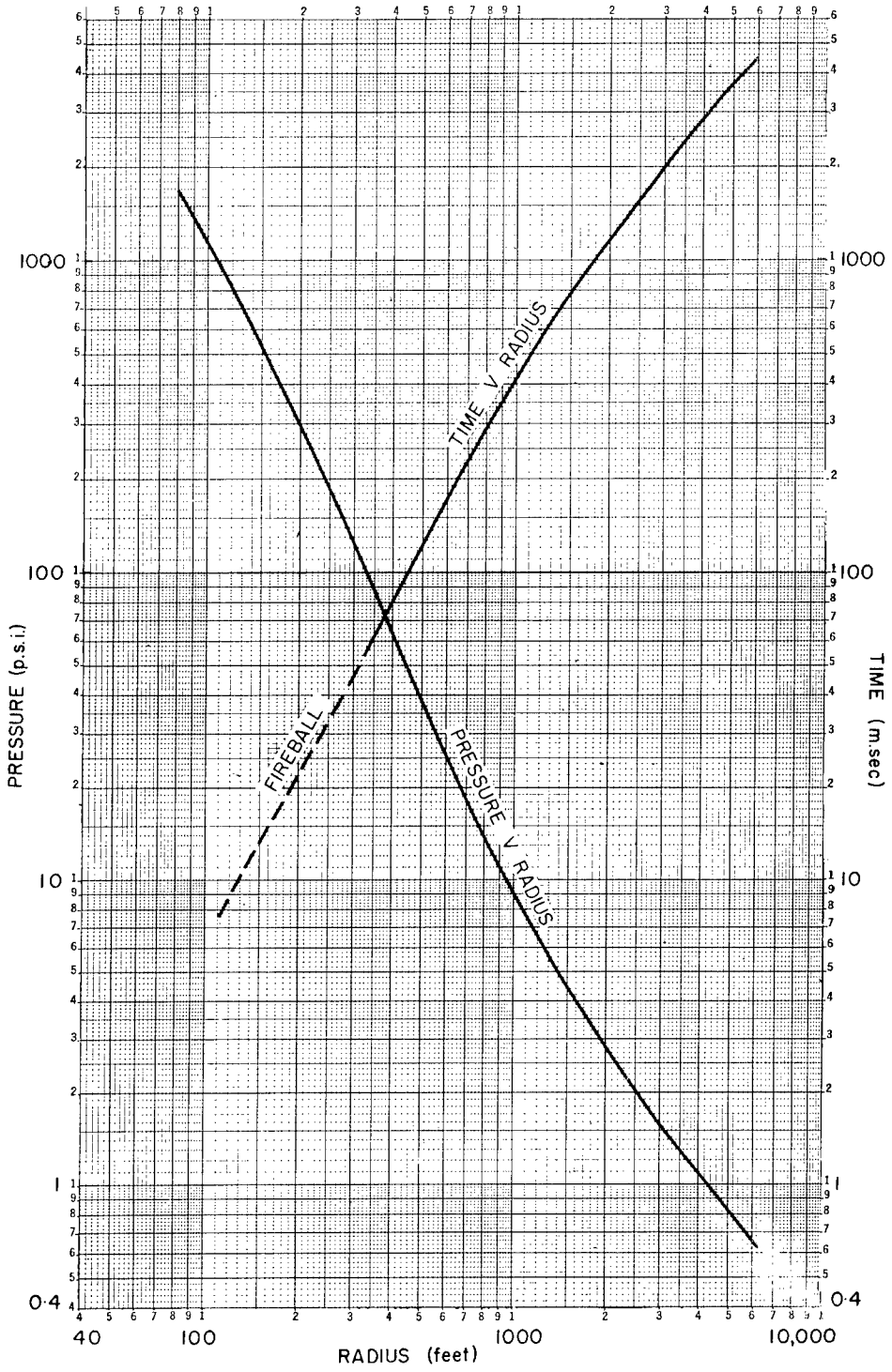

FIGURE 2. PREDICTED PRESSURE VERSUS RADIUS AND TIME VERSUS RADIUS

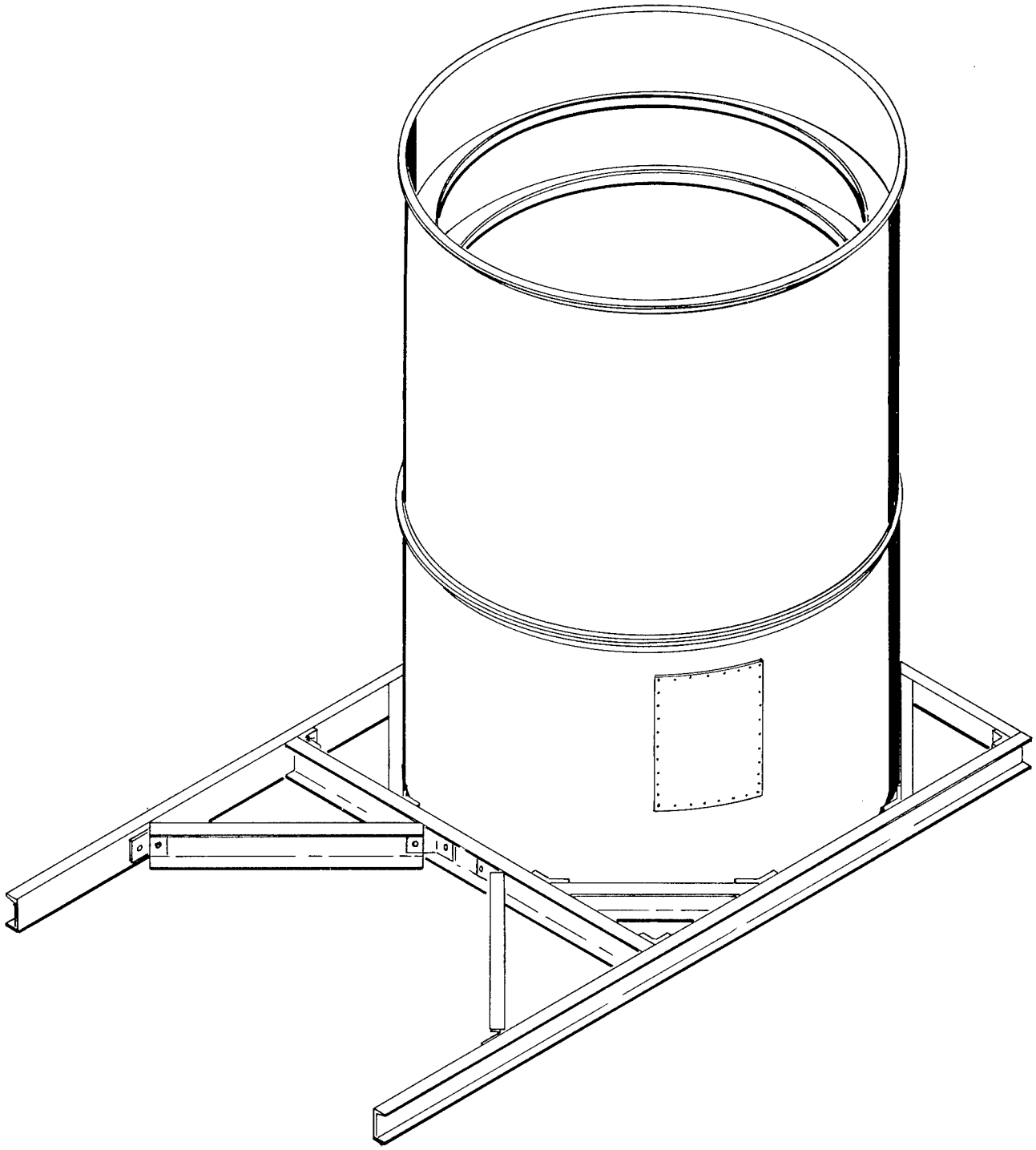

FIGURE 3. TEST CYLINDER

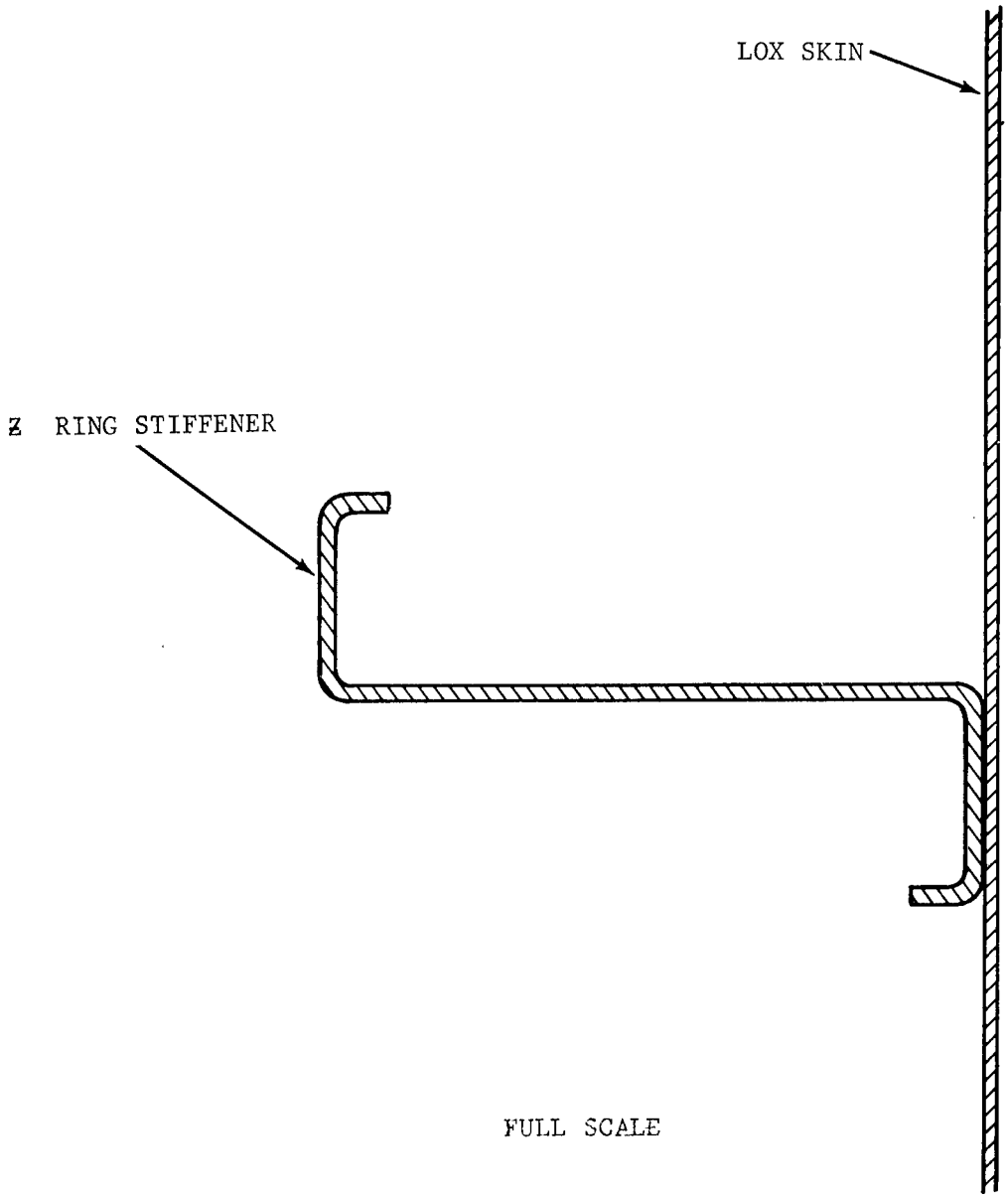

FIGURE 4. CROSS SECTION OF SKIN PANEL AND RING STIFFENER

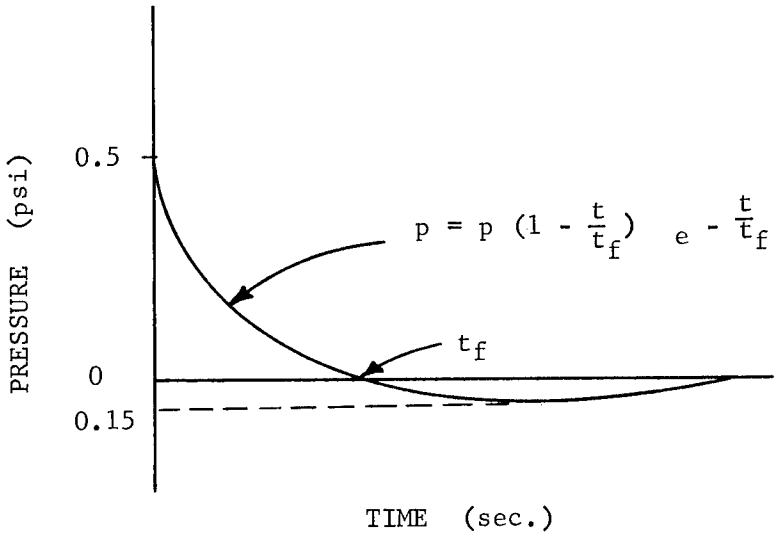

FIGURE 5. THEORETICAL PRESSURE HISTORY

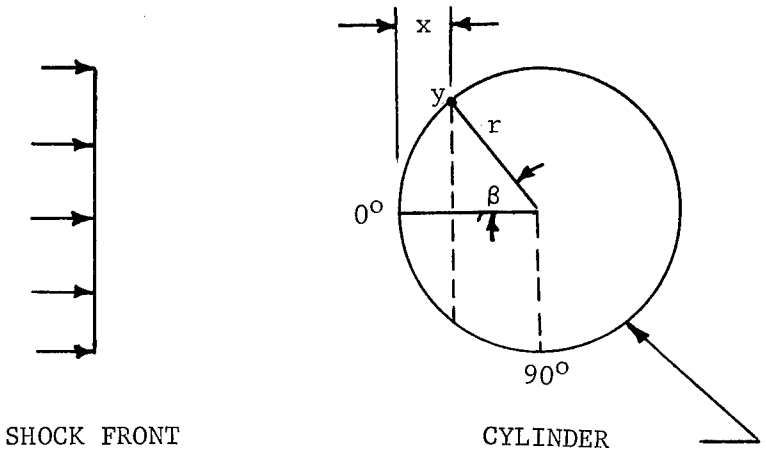

FIGURE 6. THEORETICAL SHOCK ENVELOPMENT OF CYLINDER

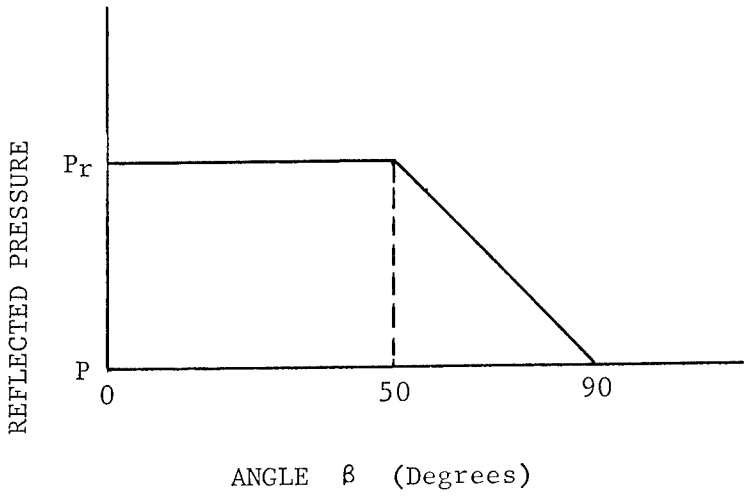

FIGURE 7. THEORETICAL REFLECTED PRESSURE

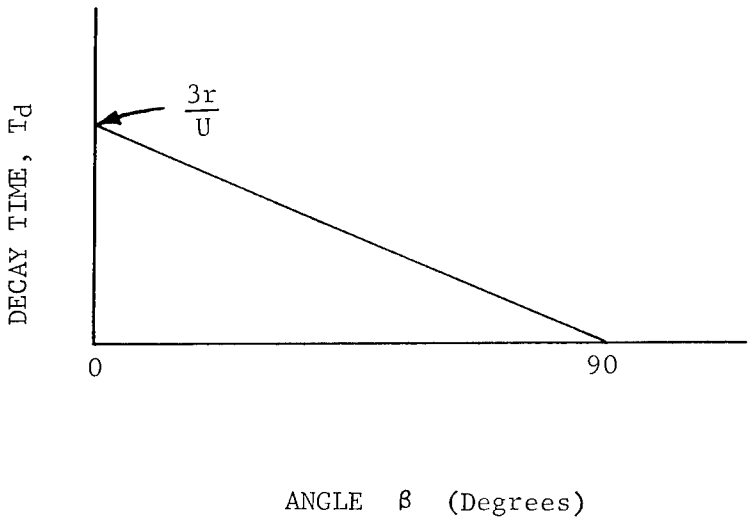

FIGURE 8. THEORETICAL DECAY TIME

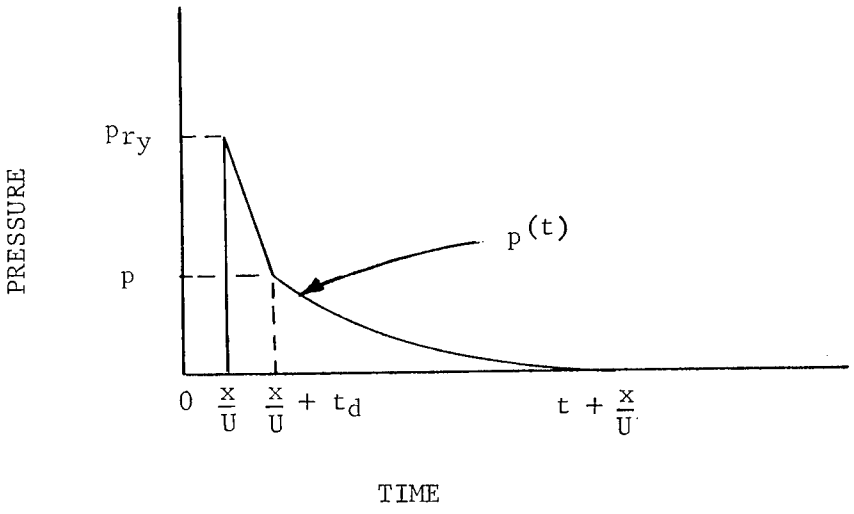

FIGURE 9. THEORETICAL REFLECTED PRESSURE

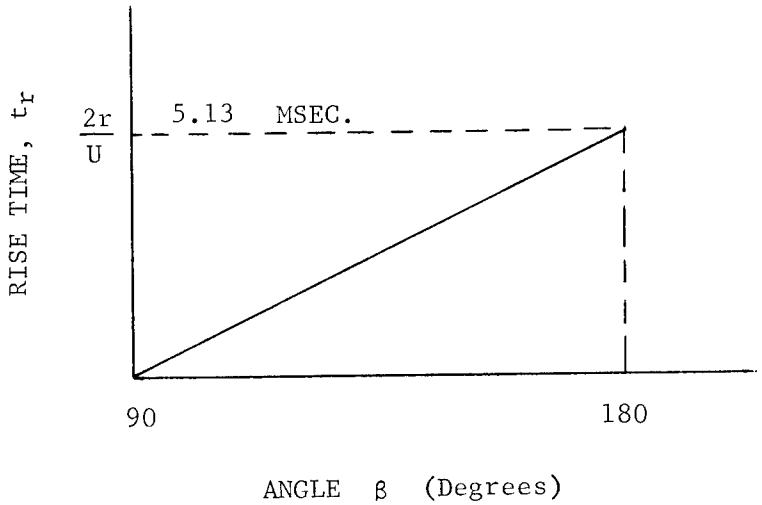

FIGURE 10. THEORETICAL RISE TIME

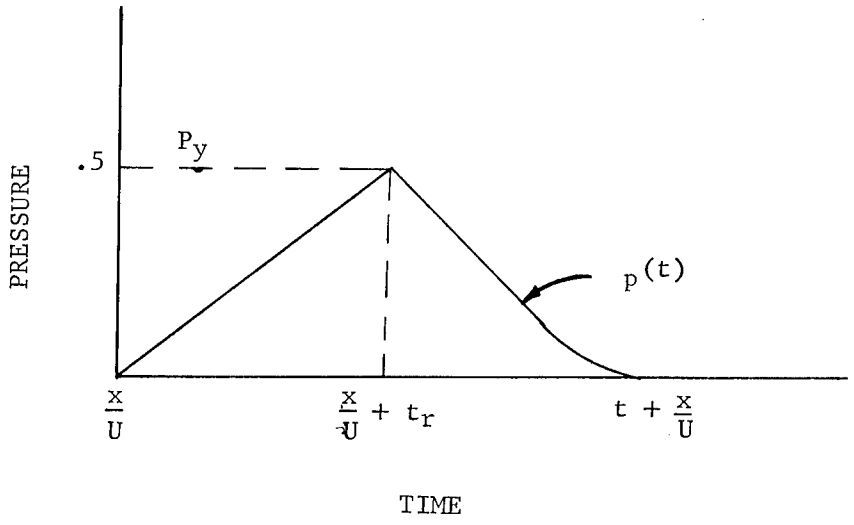

FIGURE 11. THEORETICAL PRESSURE BUILDUP

DISTANCE	OVER-PRESSURE
FT.	PSI
51.22	2930.0158
56.34	2587.0807
61.47	2298.5017
66.59	2054.6139
71.71	1847.0282
76.83	1668.9358
81.95	1514.9426
92.20	1263.1569
102.44	1067.2413
112.69	911.5491
128.05	731.6292
153.66	525.3230
179.27	390.4380
204.88	298.3218
230.49	233.2657
256.10	186.0446
281.71	150.9651
307.33	124.3766
332.94	103.8644
358.55	87.7888
384.16	75.0112
409.77	64.7249
460.99	49.4526
512.21	38.9189
563.43	31.3998
614.65	25.8733
665.87	21.7077
717.09	18.4986
768.31	15.9786
819.53	13.9661
921.98	10.9943
1024.42	8.9435
1126.86	7.4681
1280.52	5.9227
1536.63	4.3396
1792.73	3.3943
2048.83	2.7759
2304.94	2.3430
2561.04	2.0242

DISTANCE	OVER-PRESSURE
FT.	PSI
2817.15	1.7798
3073.25	1.5865
3329.36	1.4296
3585.46	1.2996
3841.56	1.1900
4097.67	1.0962
4609.88	.9440
5122.09	.8256
5634.29	.7308
6146.50	.6533
6658.71	.5886
7170.92	.5341
7683.13	.4857
8195.34	.4436
9219.76	.3759
10244.2	.3241
11268.6	.2834
12805.2	.2368
15366.3	.1832
17927.3	.1475
20488.3	.1222
23049.4	.1036
25610.4	.0893
28171.5	.0781
30732.5	.0691
33293.6	.0618
35854.6	.0556
38415.6	.0505
40976.7	.0461
46098.8	.0391
51220.9	.0337
56342.9	.0295
61465.0	.0260
66587.1	.0233
71709.2	.0210
76831.3	.0191
81953.4	.0174
92197.6	.0147
102442.	.0127

P =13.67 (Atmospheres)

FIGURE 12. PREDICTED OVERPRESSURE VERSUS DISTANCE (TABLE)

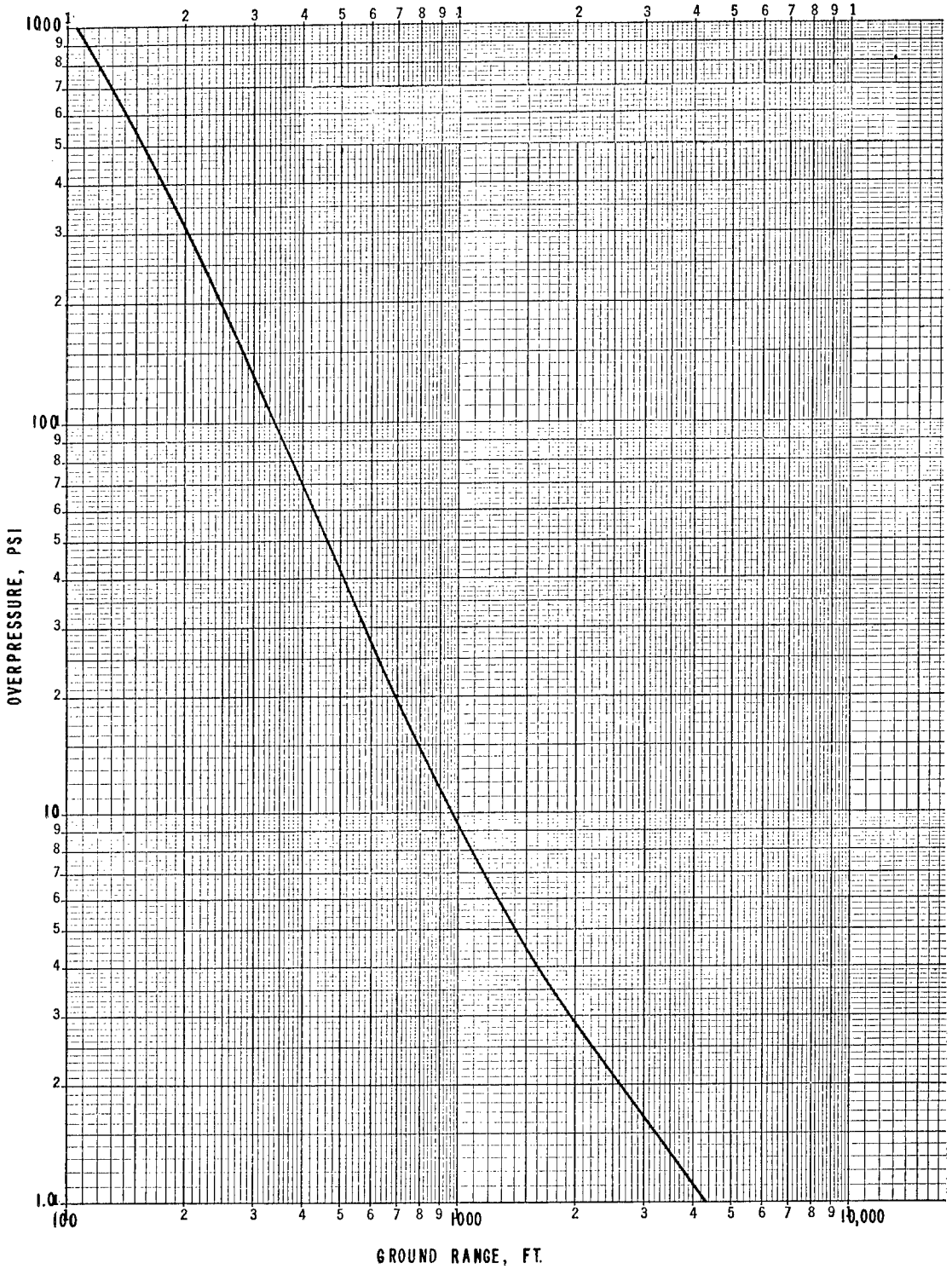

FIGURE 13. PREDICTED OVERPRESSURE VERSUS DISTANCE (CURVE)

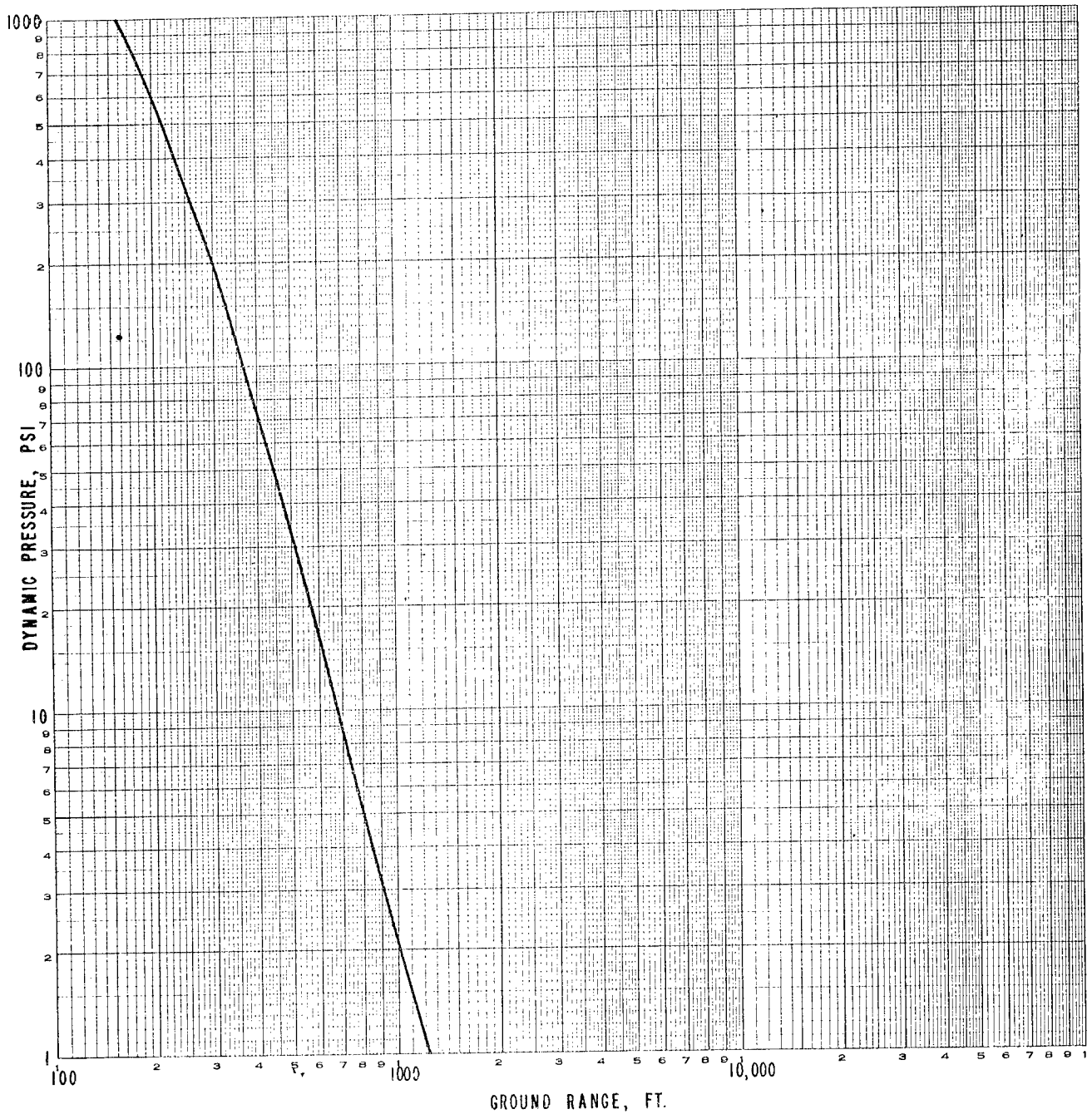

FIGURE 14. PREDICTED DYNAMIC PRESSURE

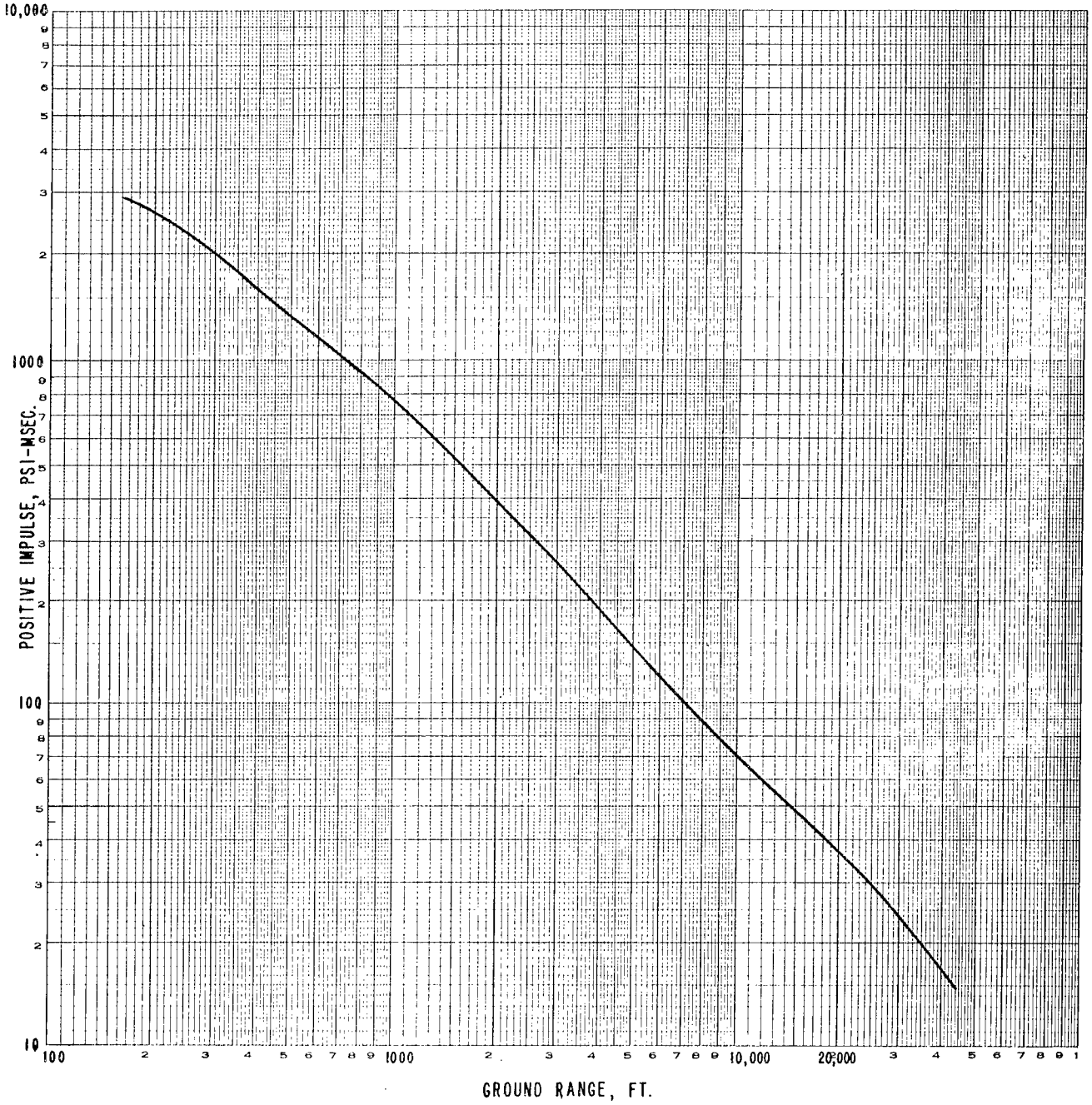

FIGURE 15. PREDICTED POSITIVE DURATION VERSUS DISTANCE

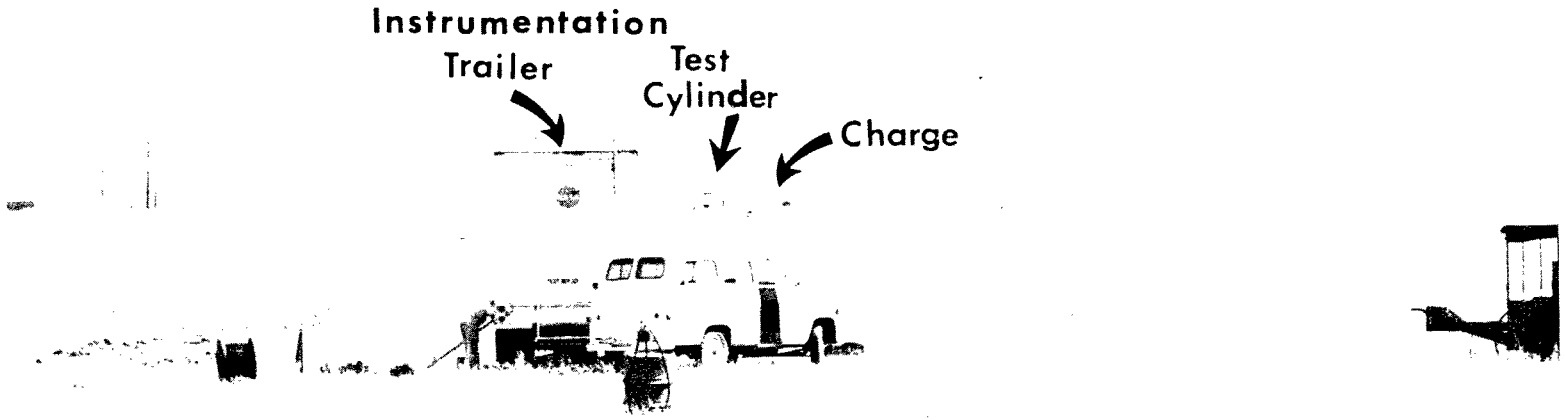

FIGURE 16. VIEW OF OVERALL TEST SETUP

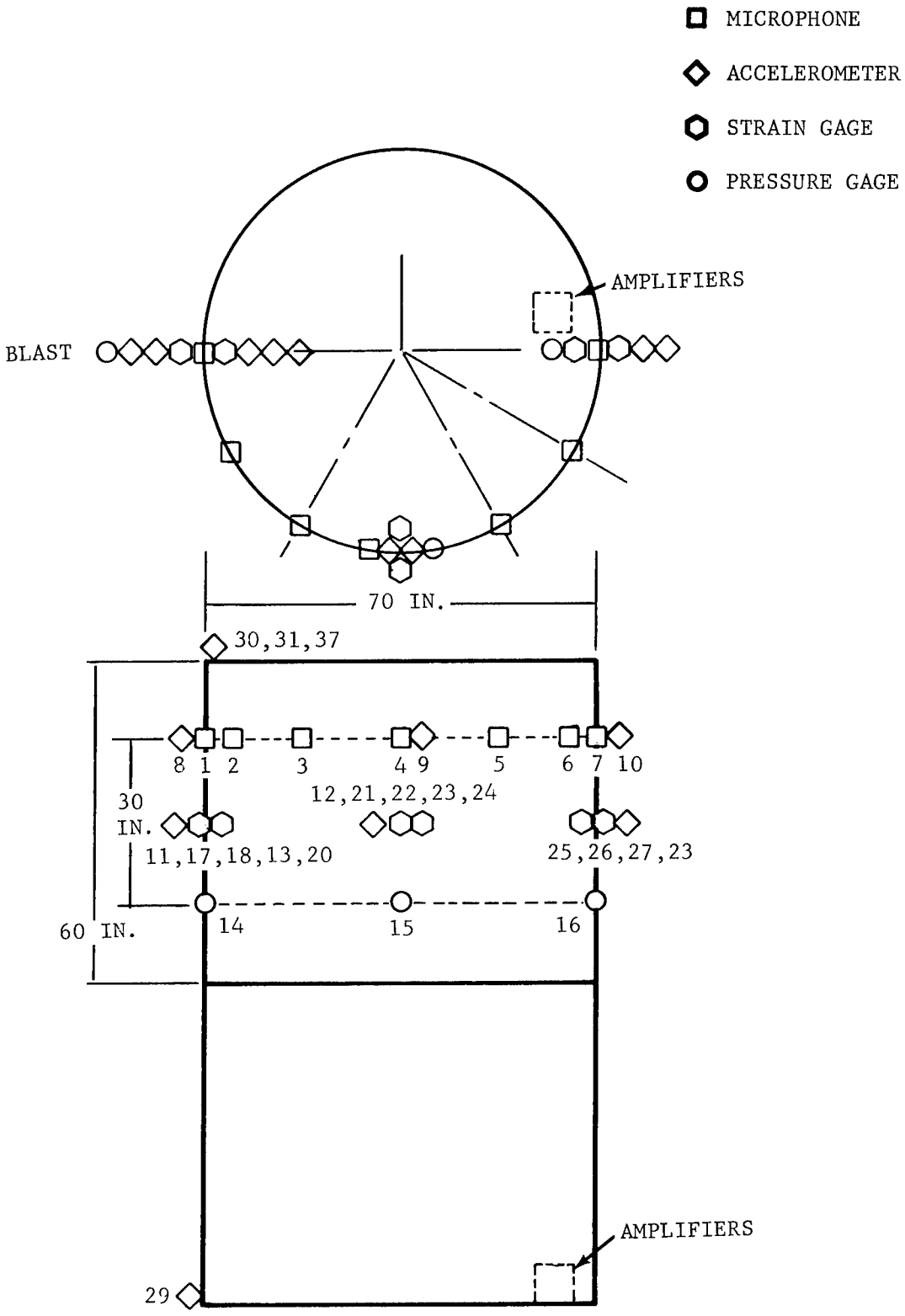

FIGURE 17. MEASUREMENT LOCATIONS ON CYLINDER

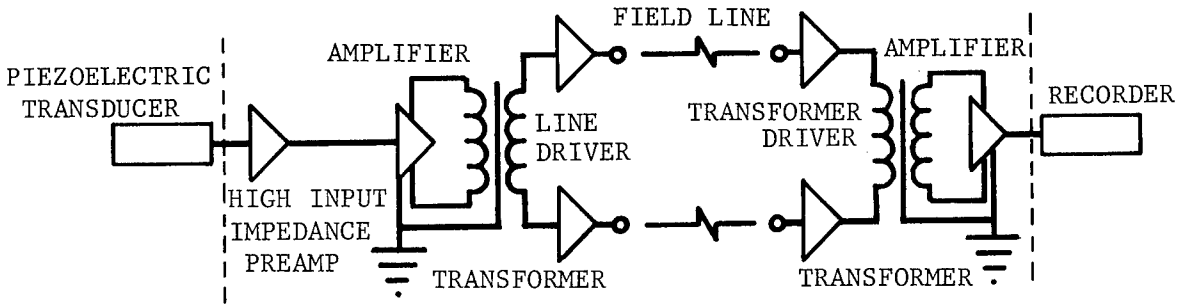

FIGURE 18. MICROPHONE AND ACCELEROMETER MEASURING SYSTEM BLOCK DIAGRAM

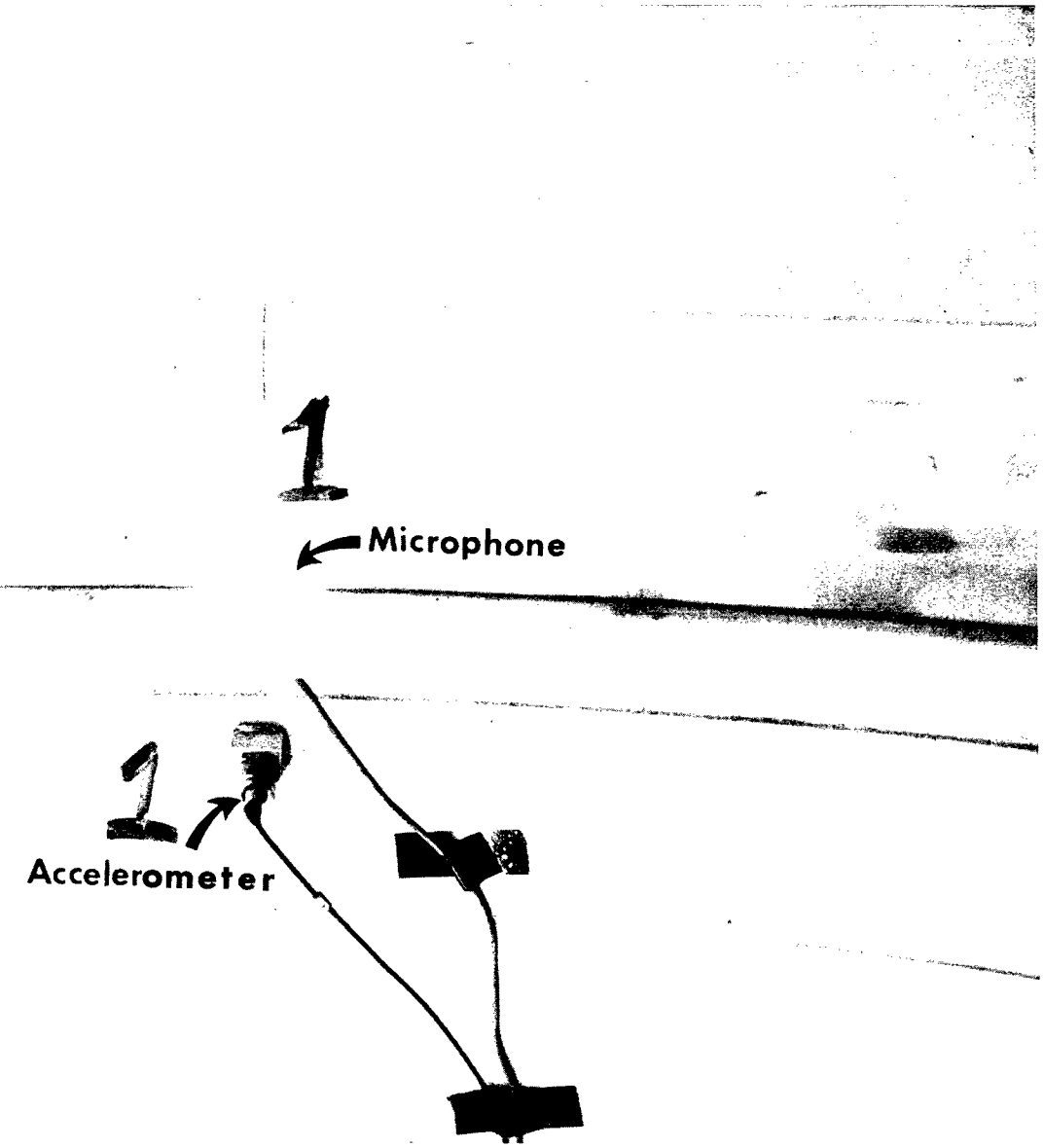

FIGURE 19. TYPICAL MICROPHONE AND ACCELEROMETER LOCATION

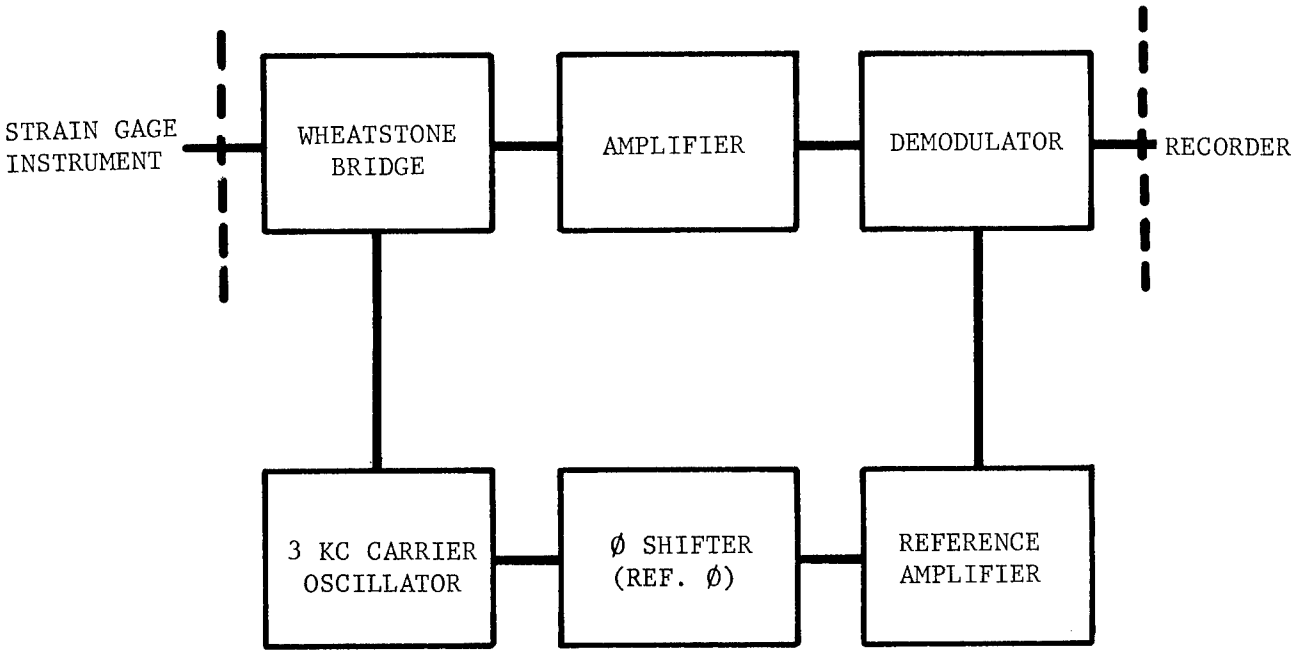

FIGURE 20. STRAIN GAGE MEASURING SYSTEM BLOCK DIAGRAM

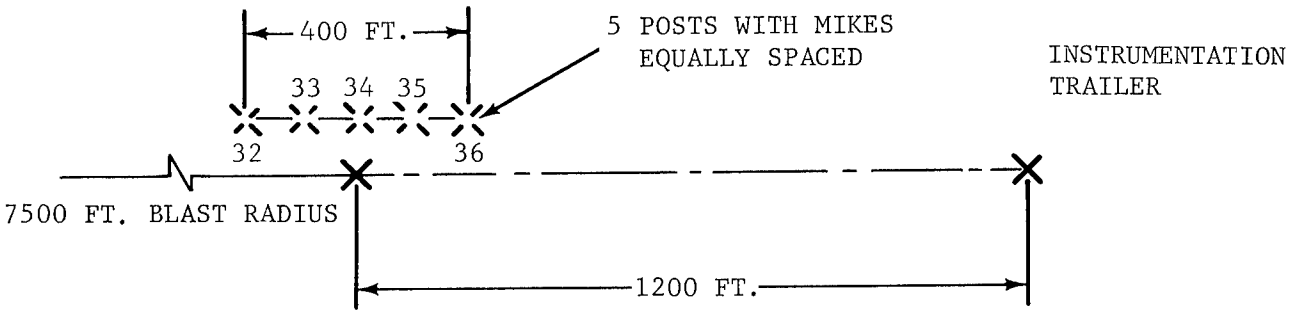

FIGURE 21. MEASUREMENT LOCATIONS ON BLAST RADIUS

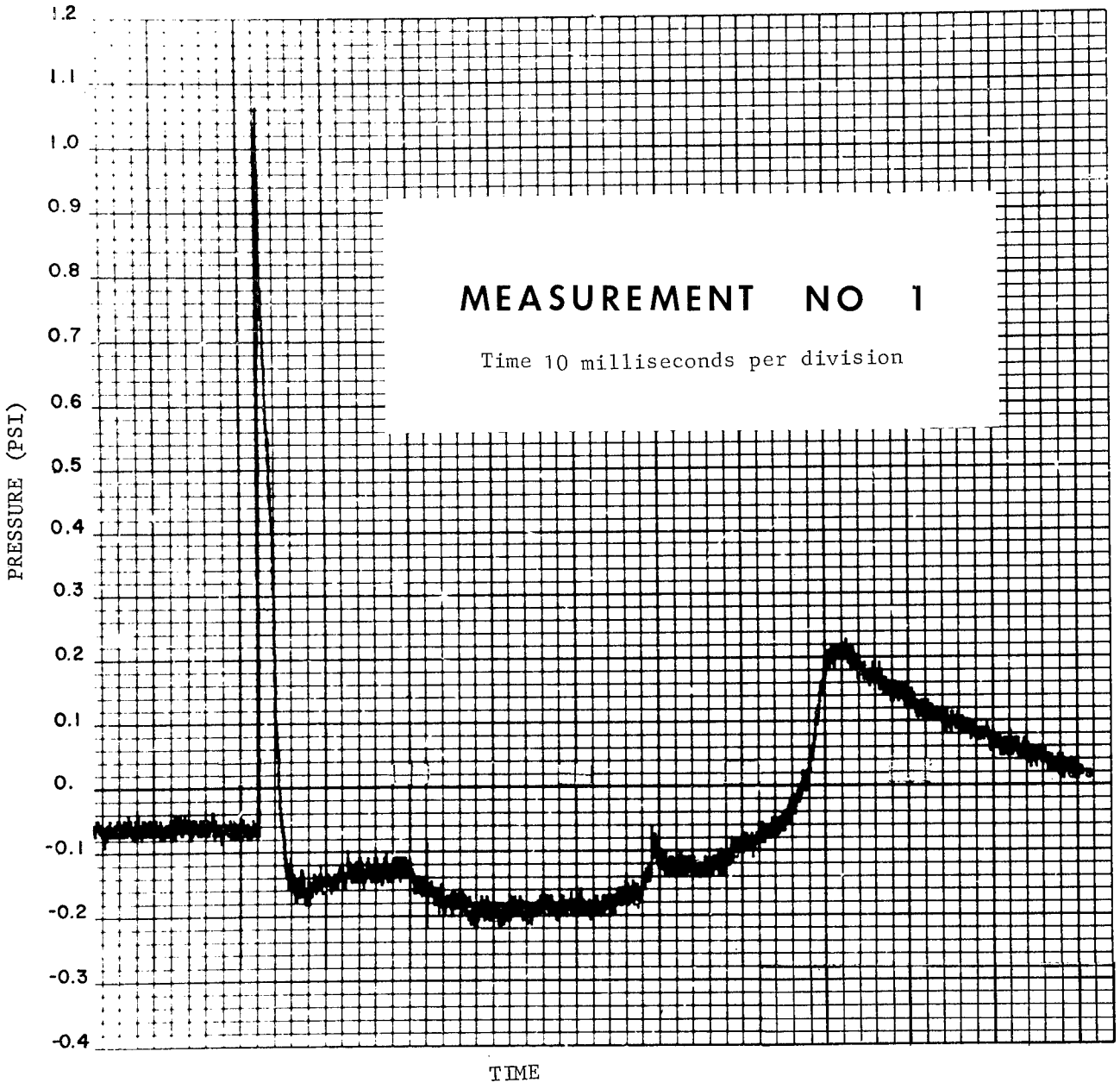

FIGURE 22. TEST DATA, CYLINDER PRESSURE MEASUREMENT NO. 1

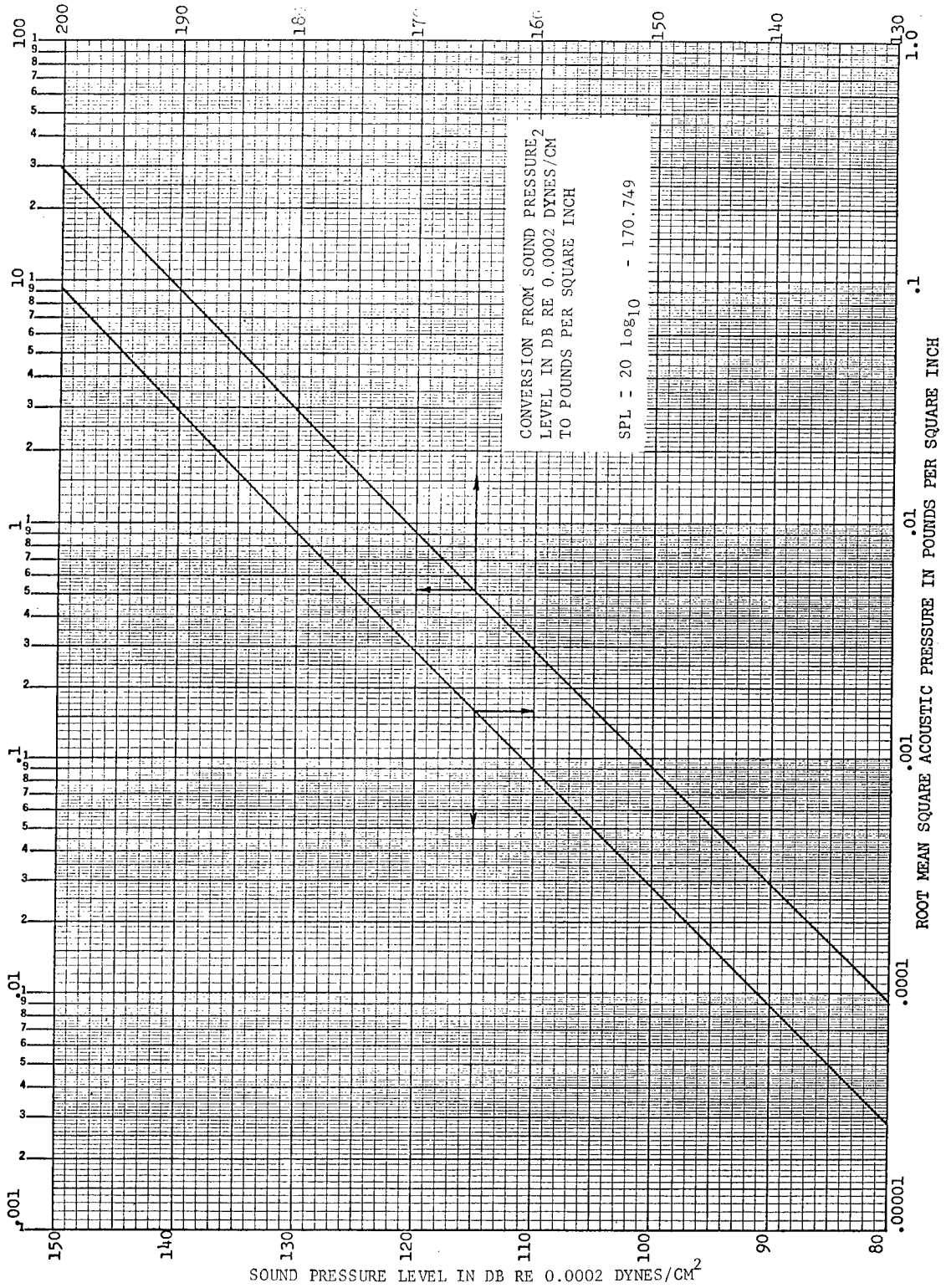

FIGURE 23. db TO psi CONVERSION CHART

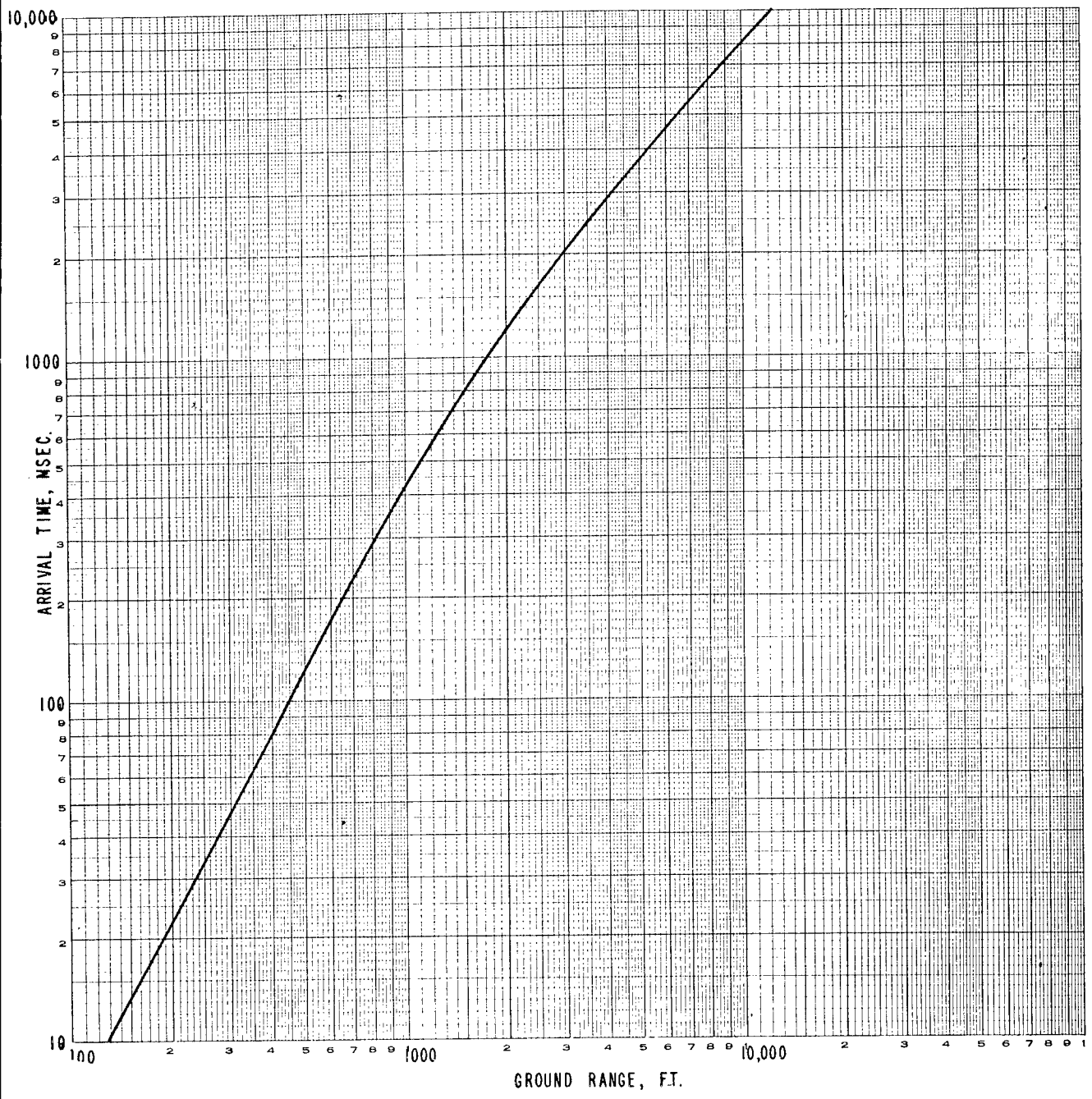

FIGURE 24. PREDICTED ARRIVAL TIME VERSUS DISTANCE

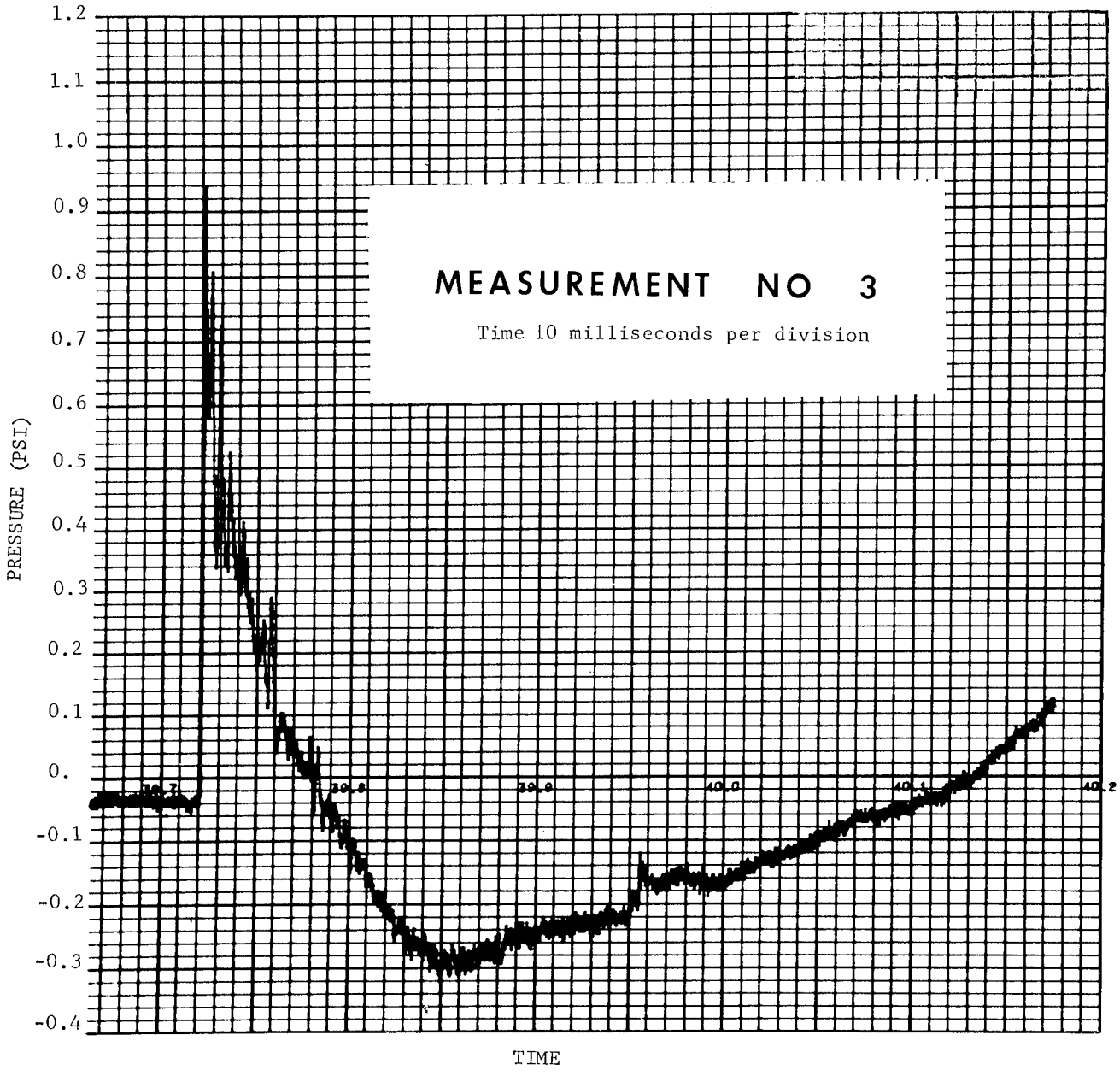

FIGURE 25. TEST DATA, CYLINDER PRESSURE MEASUREMENT NO. 3

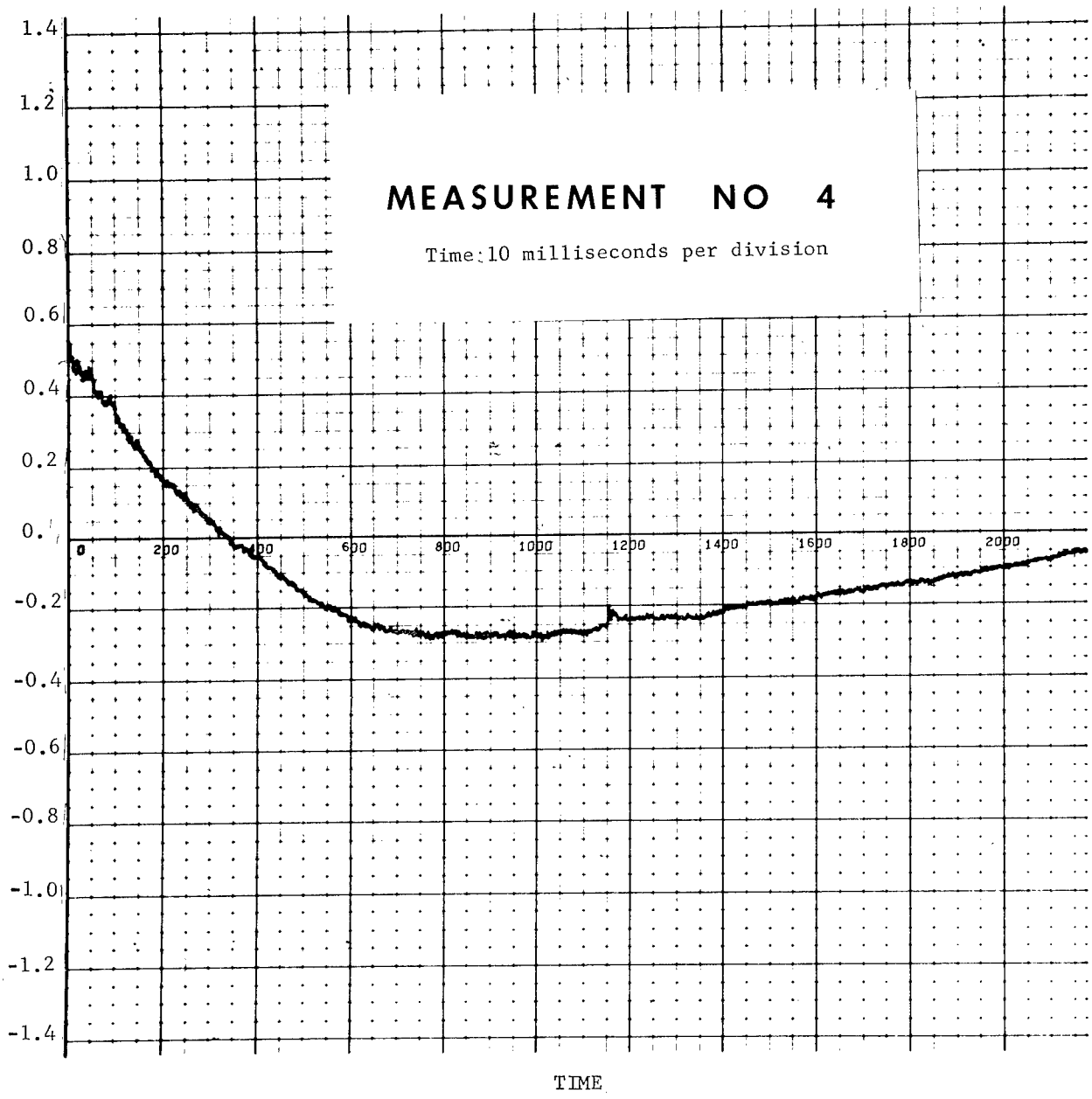

FIGURE 26. TEST DATA, CYLINDER PRESSURE MEASUREMENT NO. 4

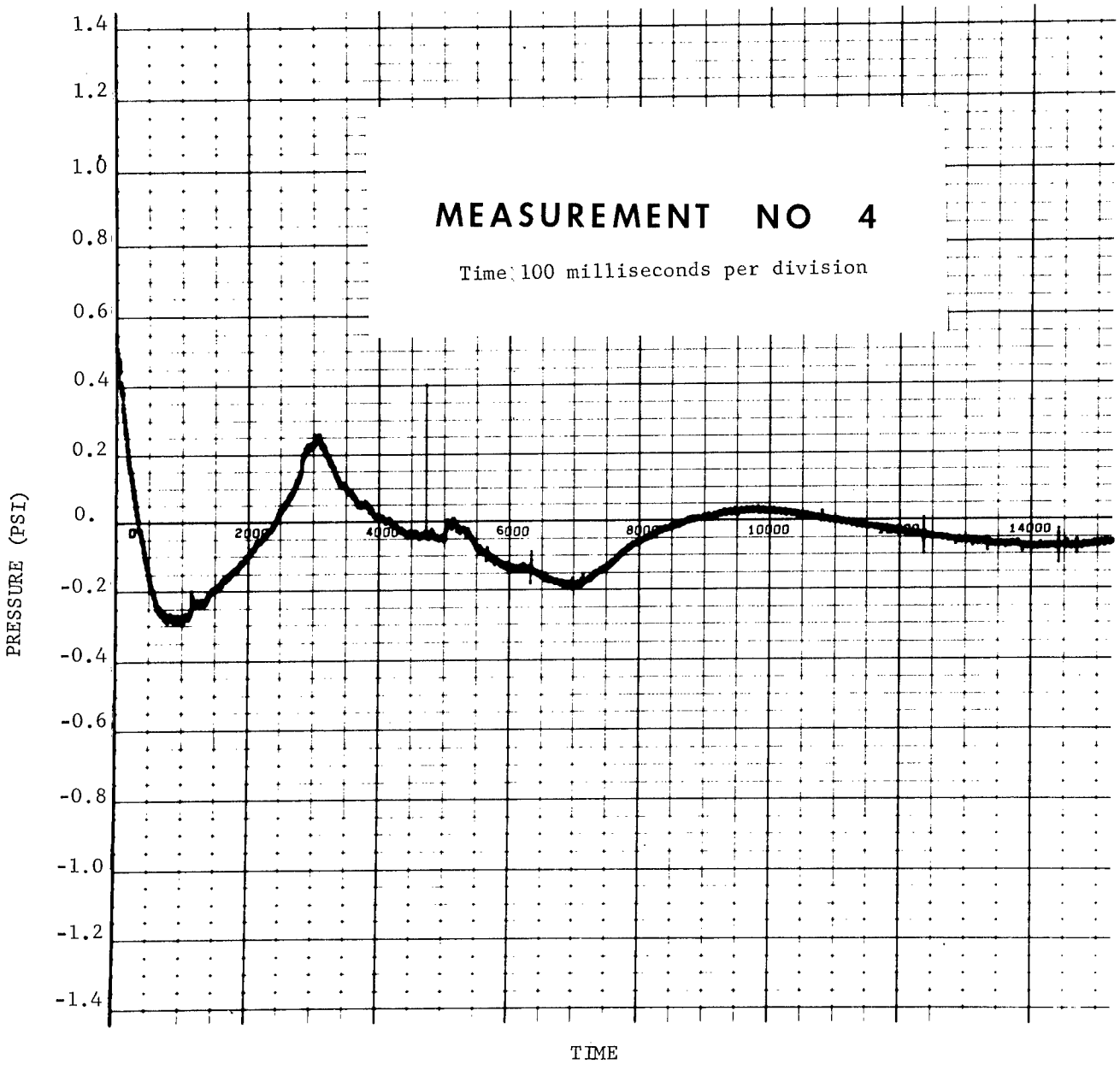

FIGURE 27. TEST DATA, CYLINDER PRESSURE MEASUREMENT NO. 4

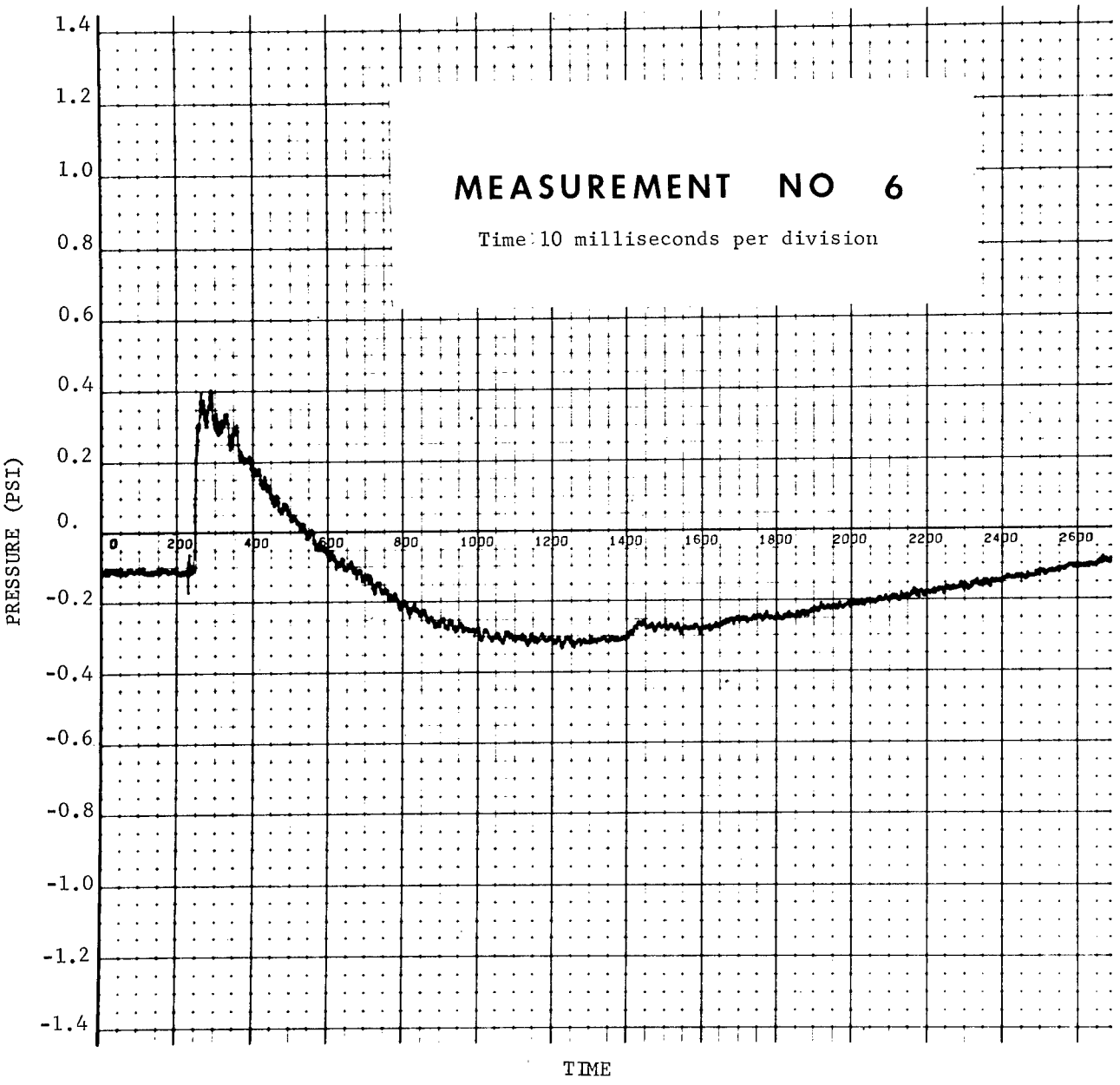

FIGURE 28. TEST DATA, CYLINDER PRESSURE MEASUREMENT NO. 6

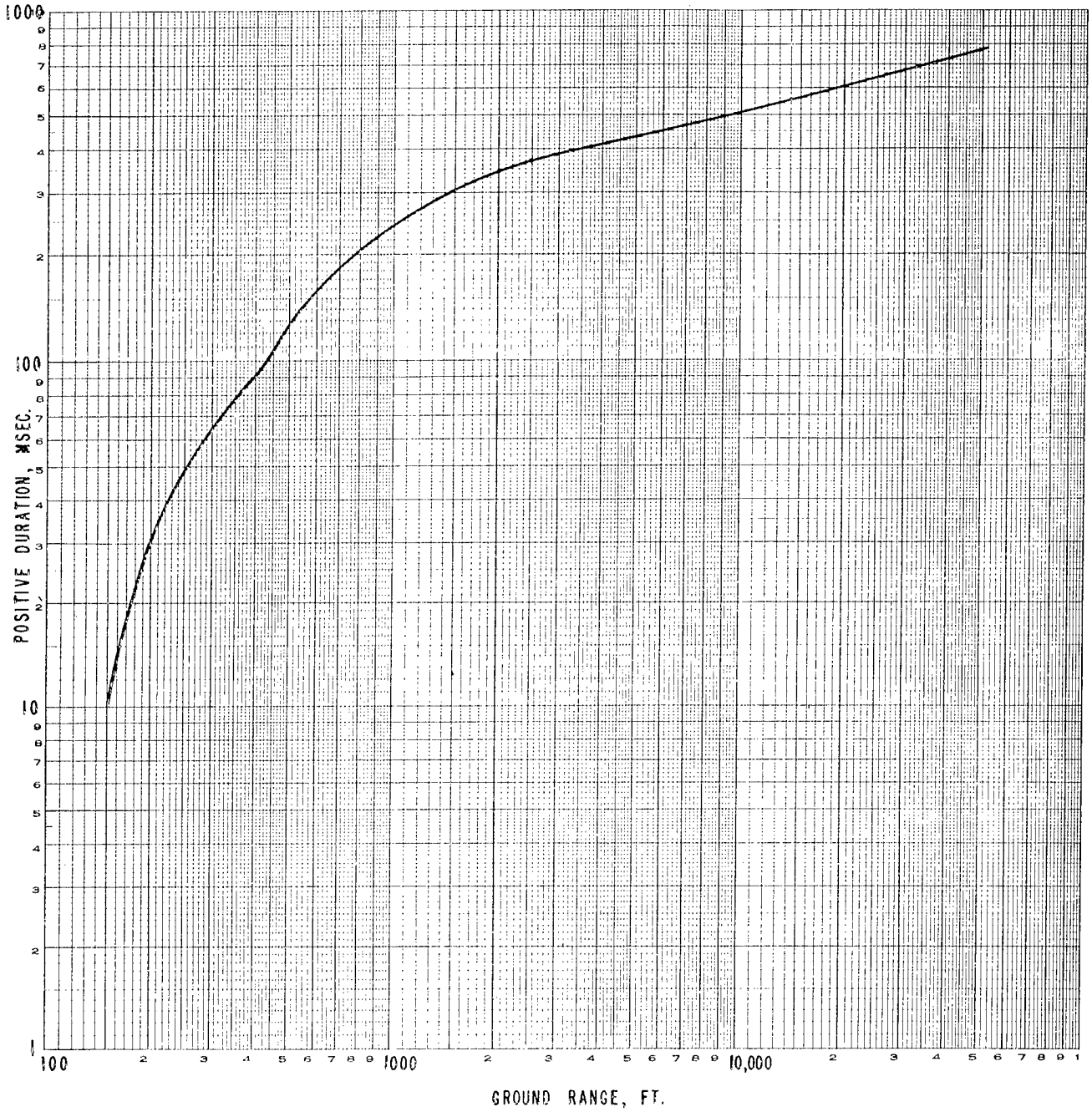

FIGURE 29. PREDICTED POSITIVE DURATION VERSUS DISTANCE

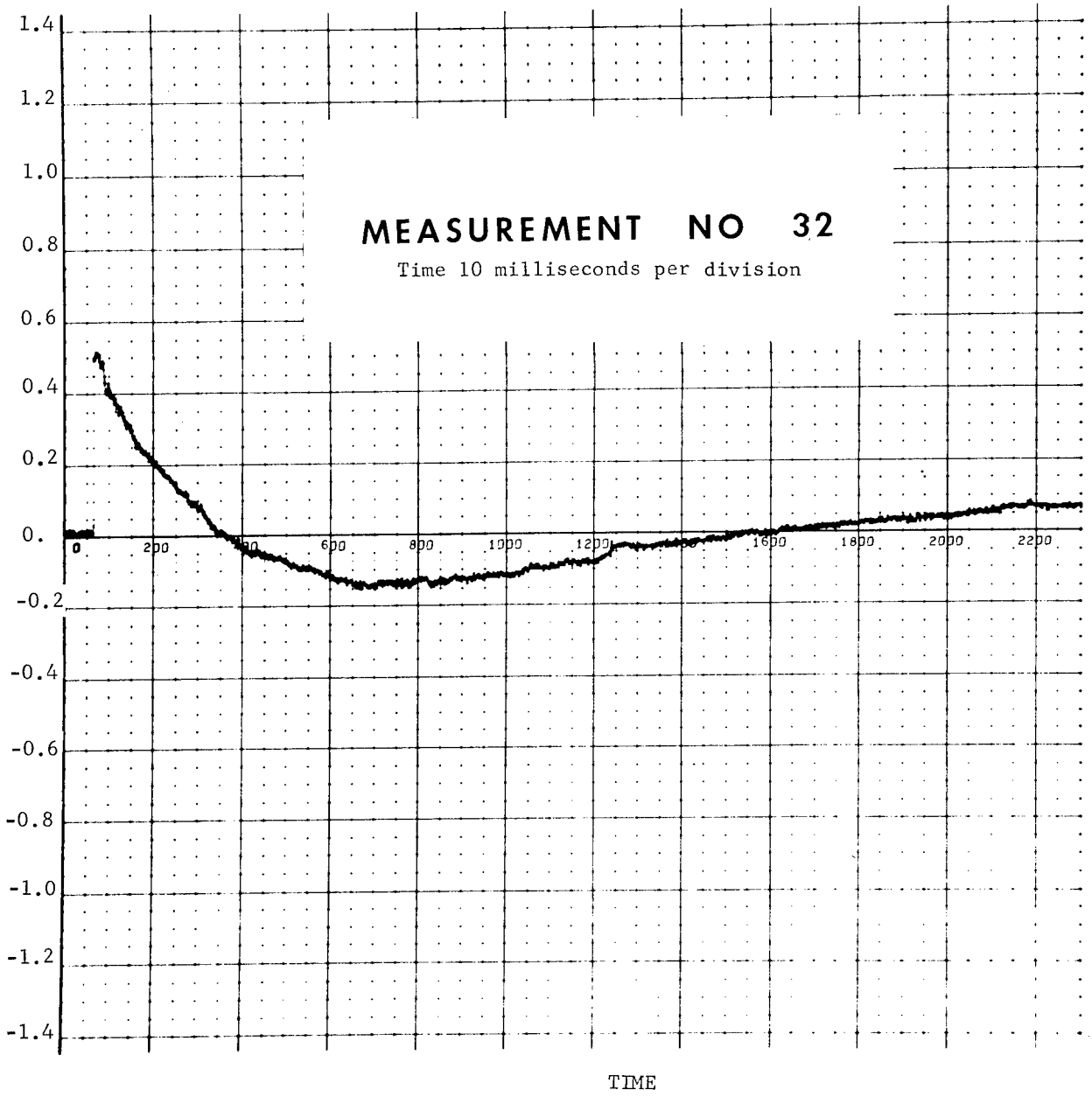

FIGURE 30. TEST DATA, FREE FIELD PRESSURE MEASUREMENT NO. 32

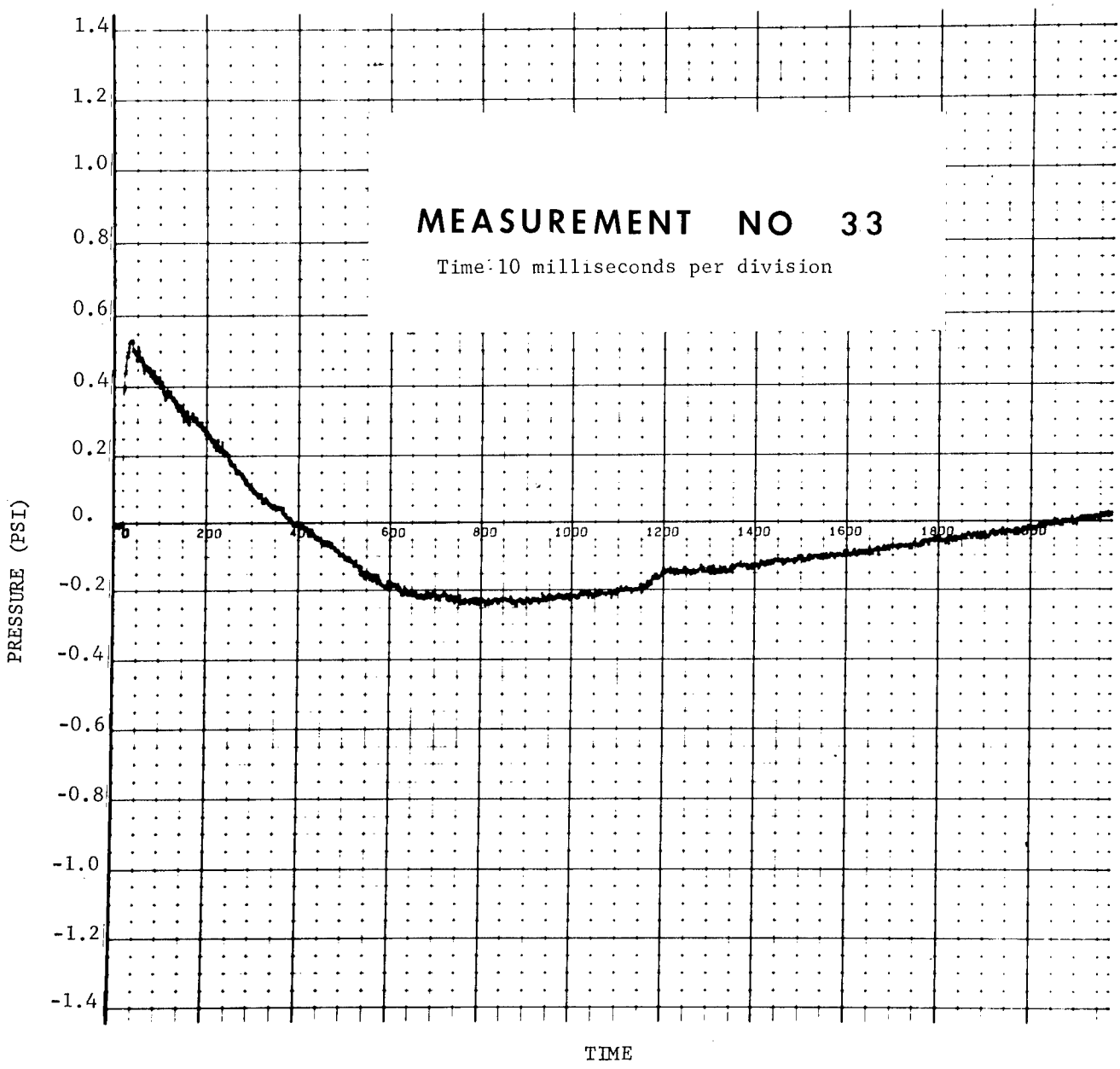

FIGURE 31. TEST DATA, FREE FIELD PRESSURE MEASUREMENT NO. 33

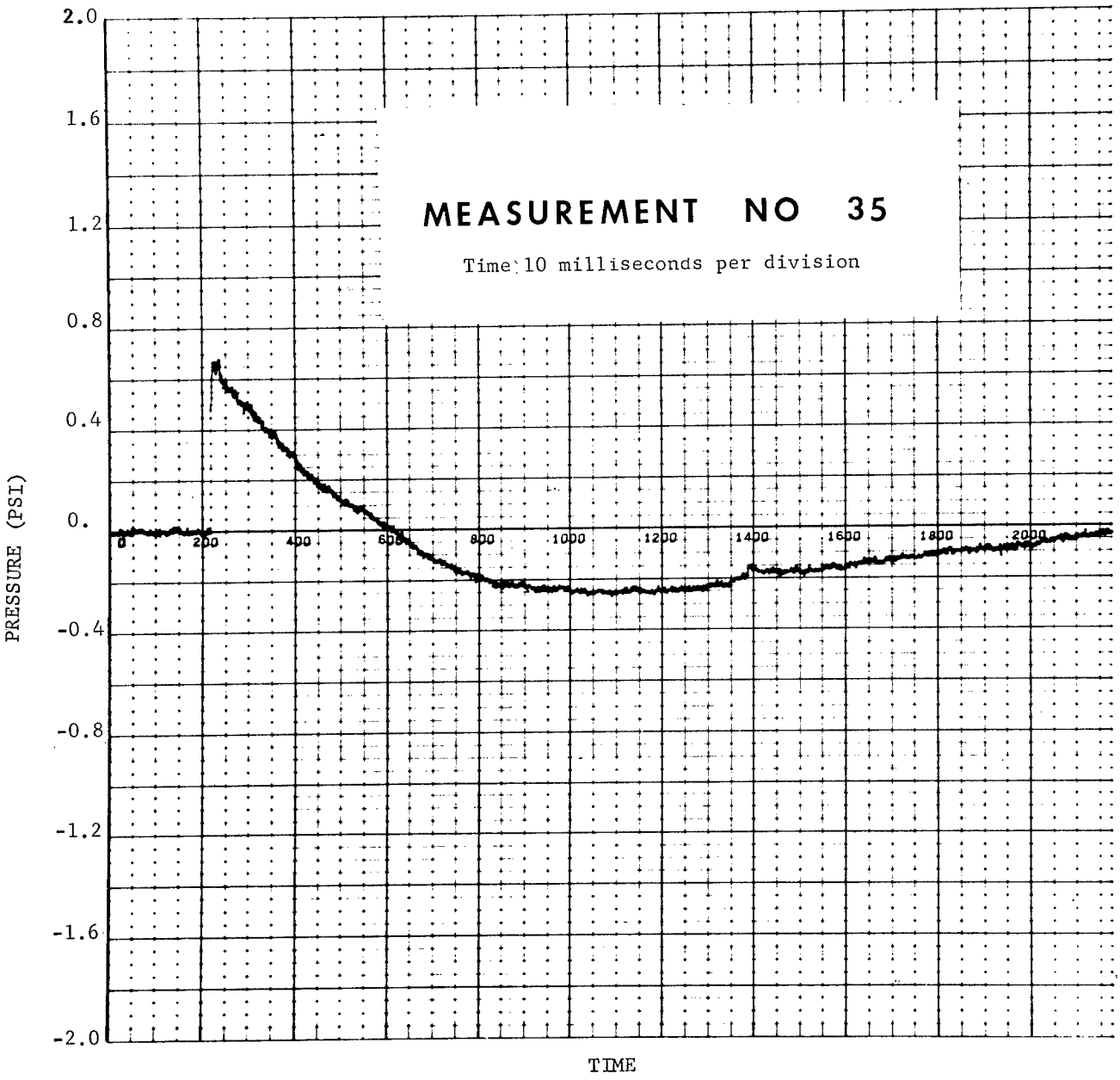

FIGURE 32. TEST DATA, FREE FIELD PRESSURE MEASUREMENT NO. 35

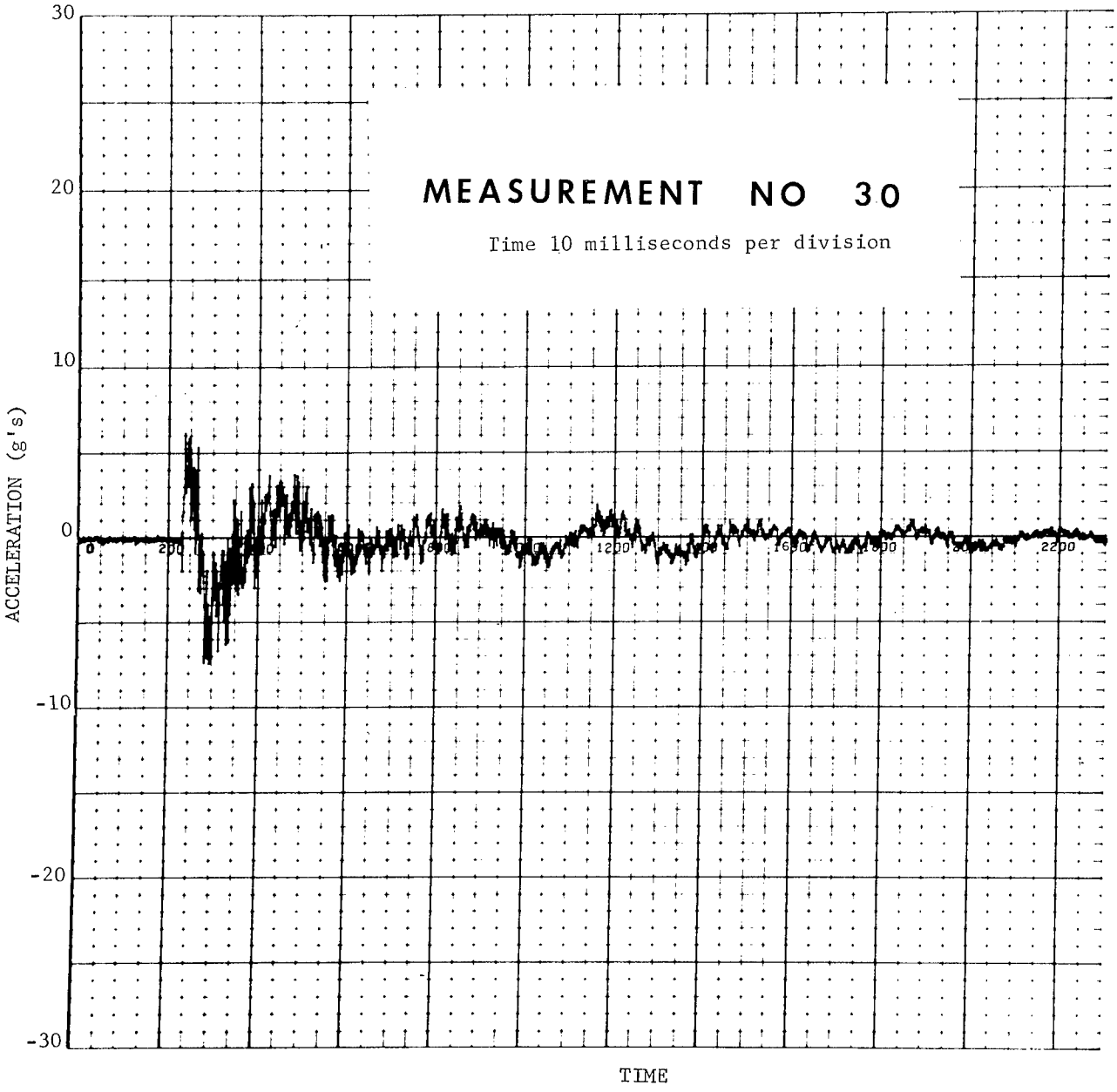

FIGURE 33. TEST DATA, OVERALL VIBRATION MEASUREMENT NO. 30

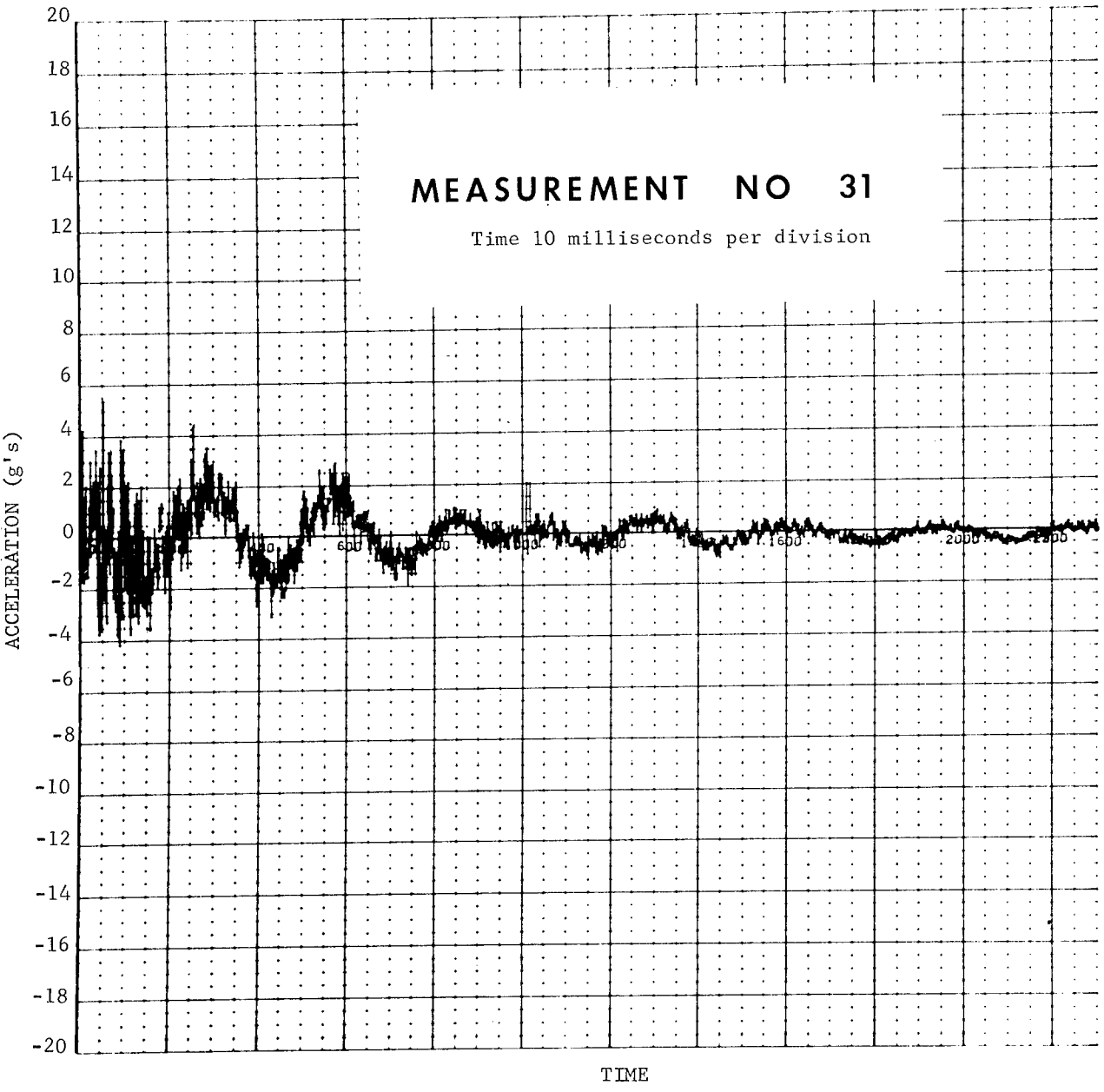

FIGURE 34. TEST DATA, OVERALL VIBRATION MEASUREMENT NO. 31

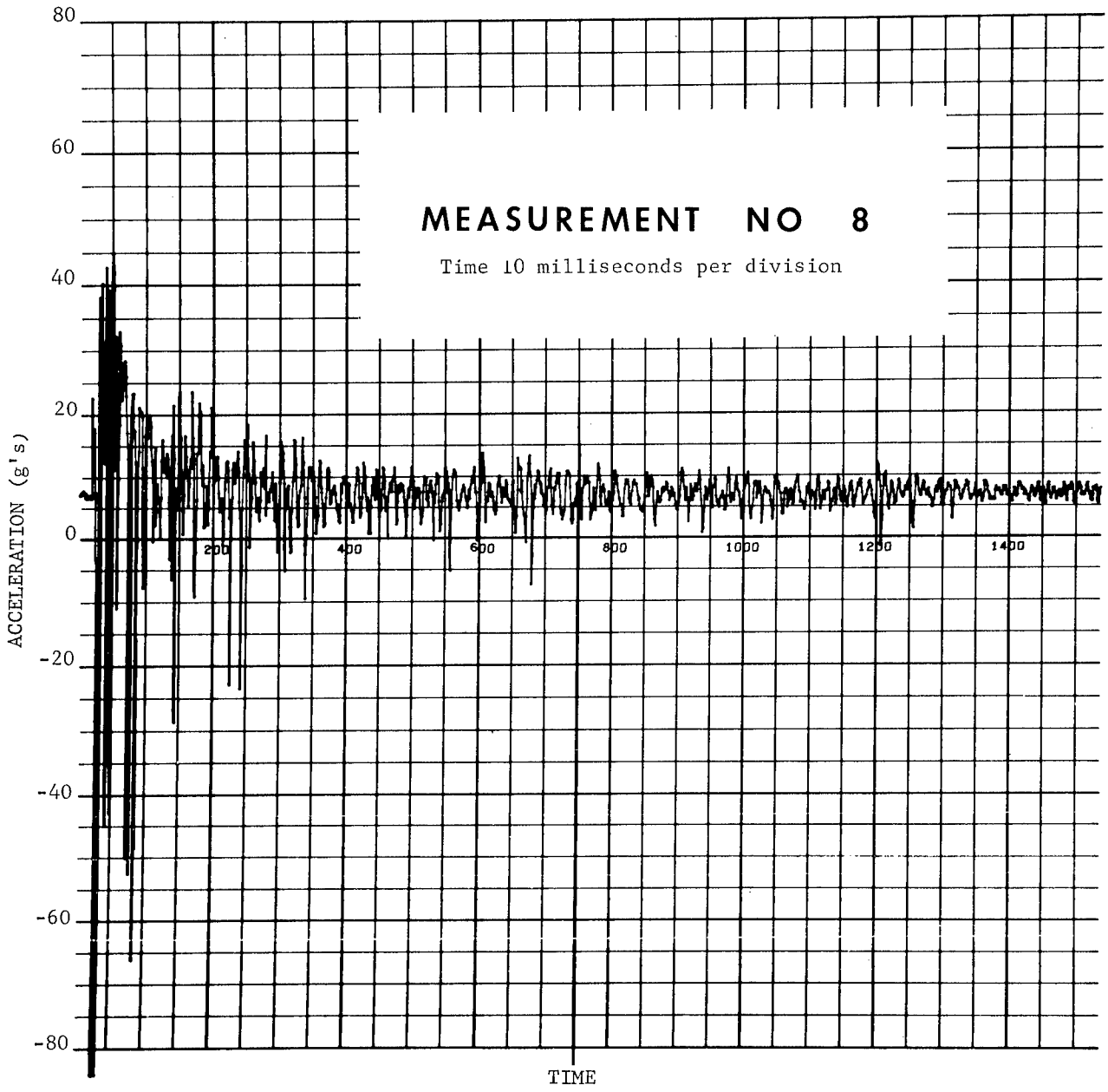

FIGURE 35. TEST DATA, LOCAL VIBRATION MEASUREMENT NO. 8

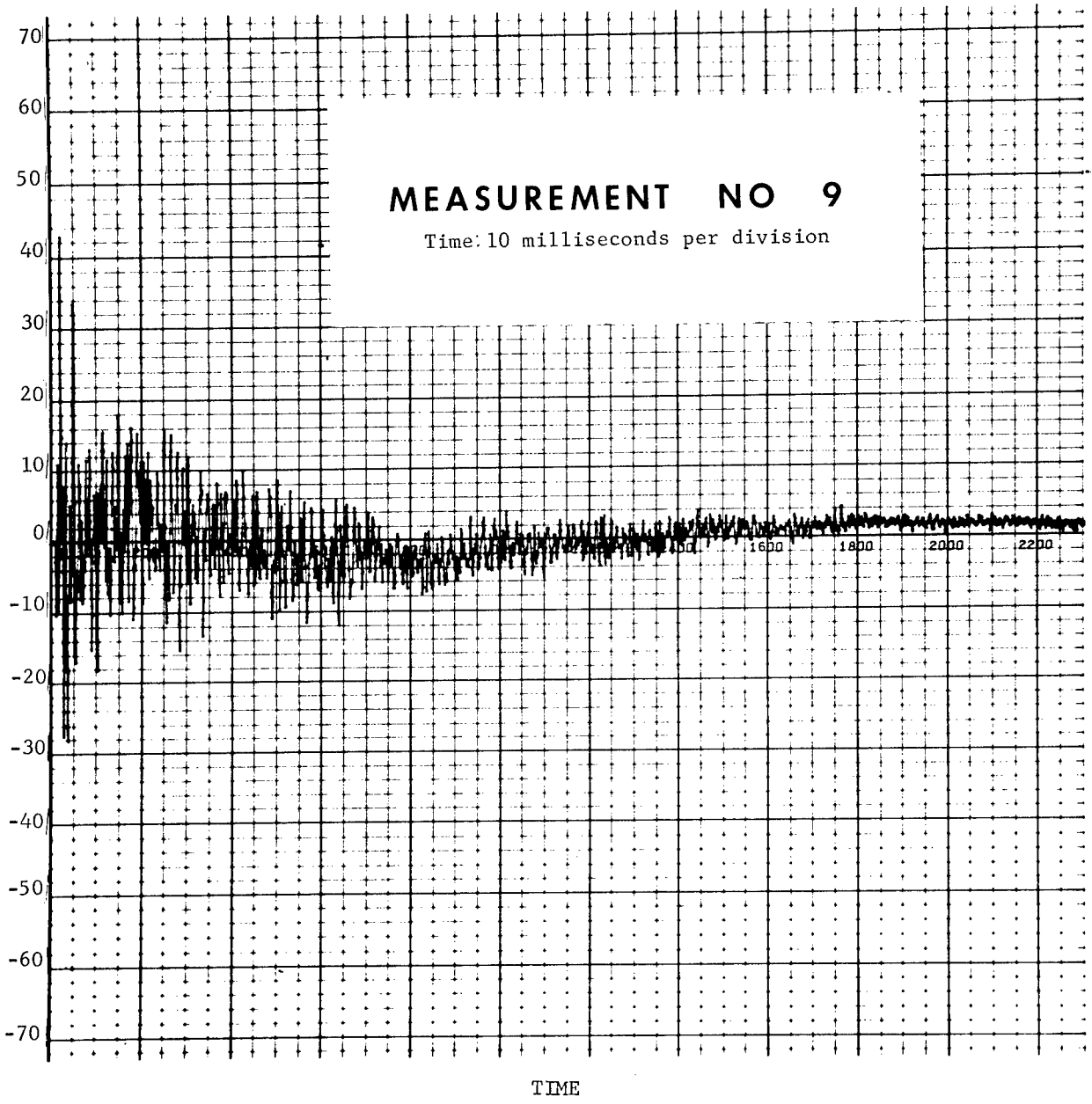

FIGURE 36. TEST DATA, LOCAL VIBRATION MEASUREMENT NO. 9

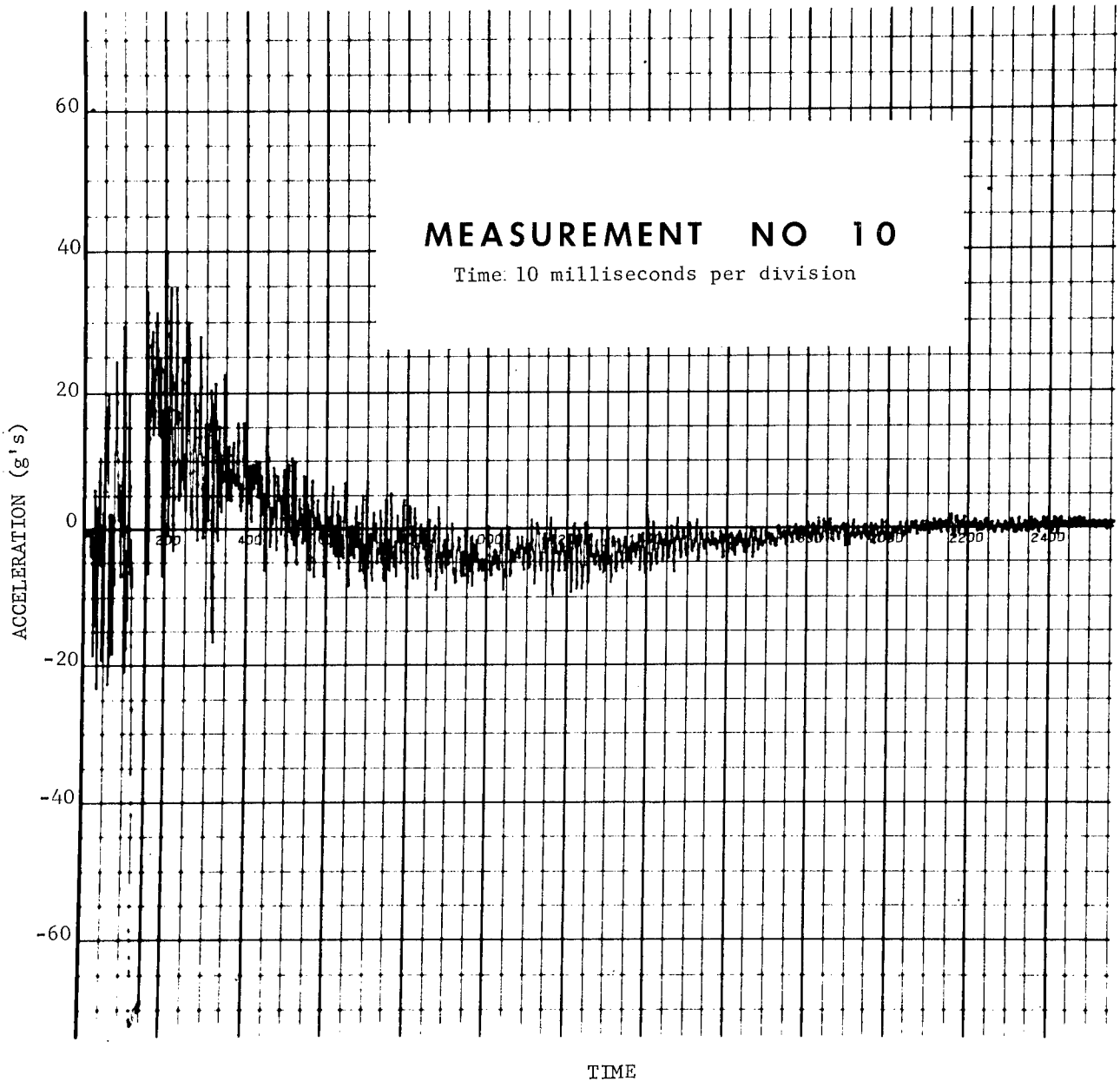

FIGURE 37. TEST DATA, LOCAL VIBRATION MEASUREMENT NO. 10

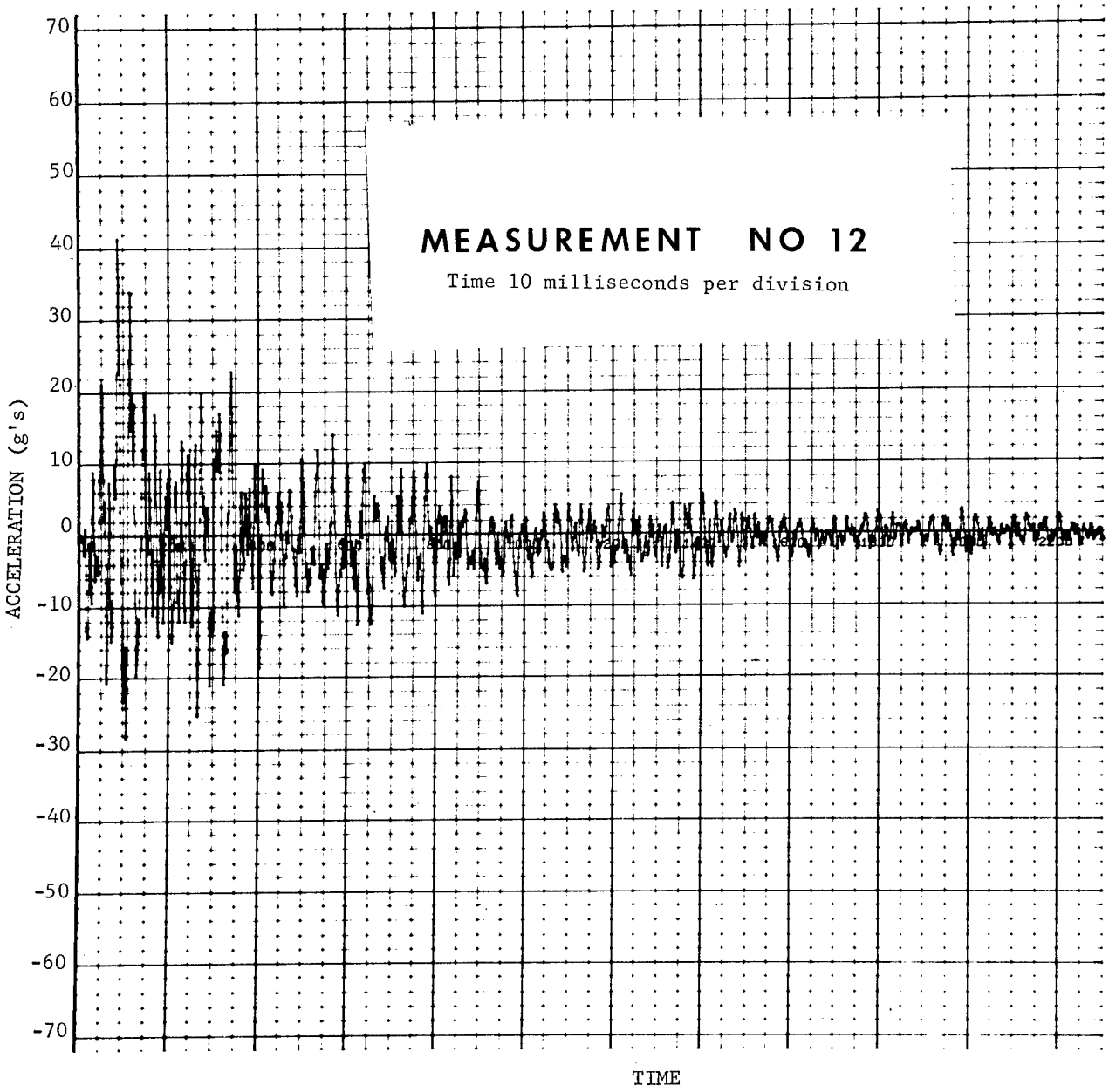

FIGURE 38. TEST DATA, LOCAL VIBRATION MEASUREMENT NO. 12

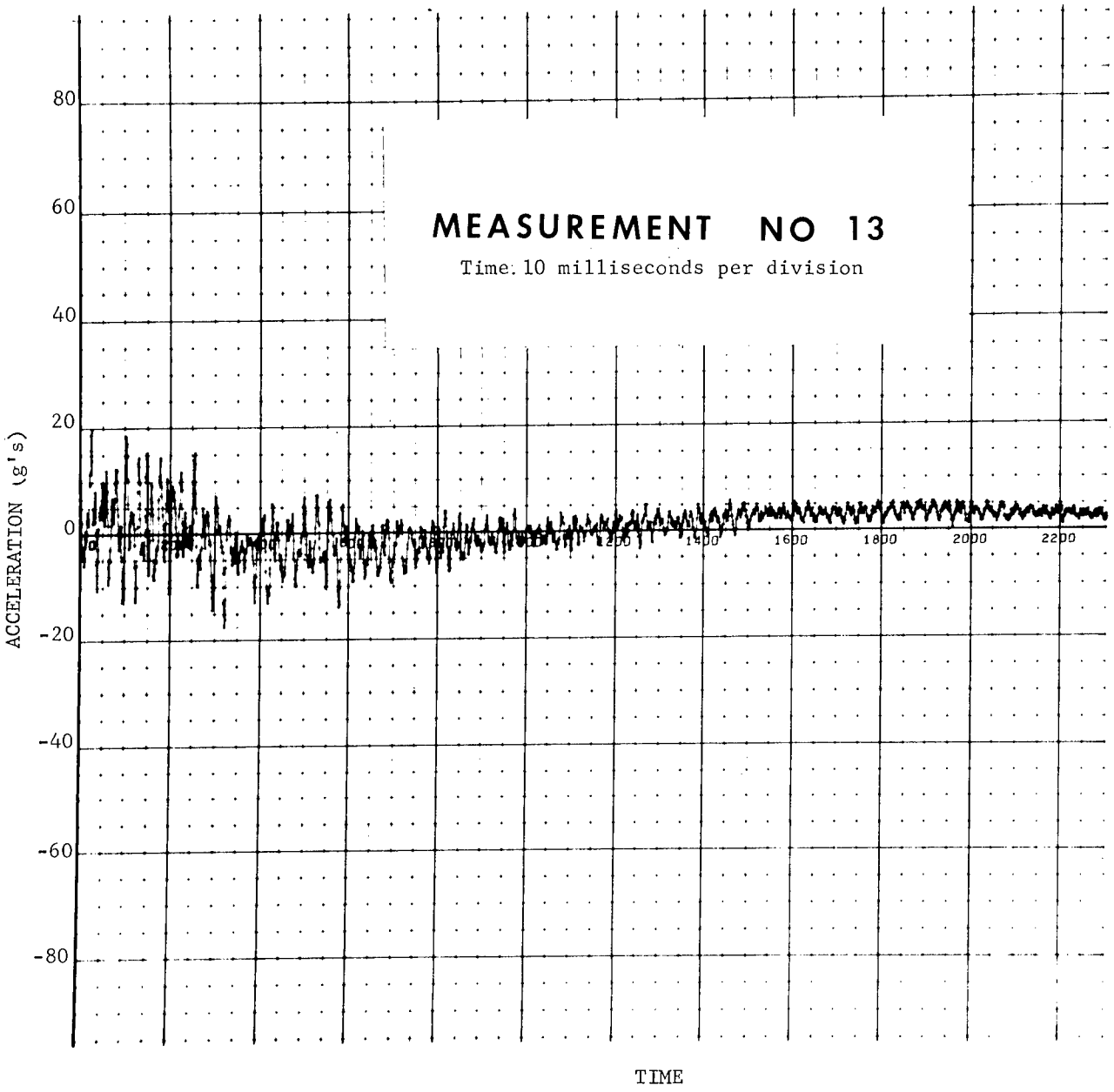

FIGURE 39. TEST DATA, LOCAL VIBRATION MEASUREMENT NO. 13

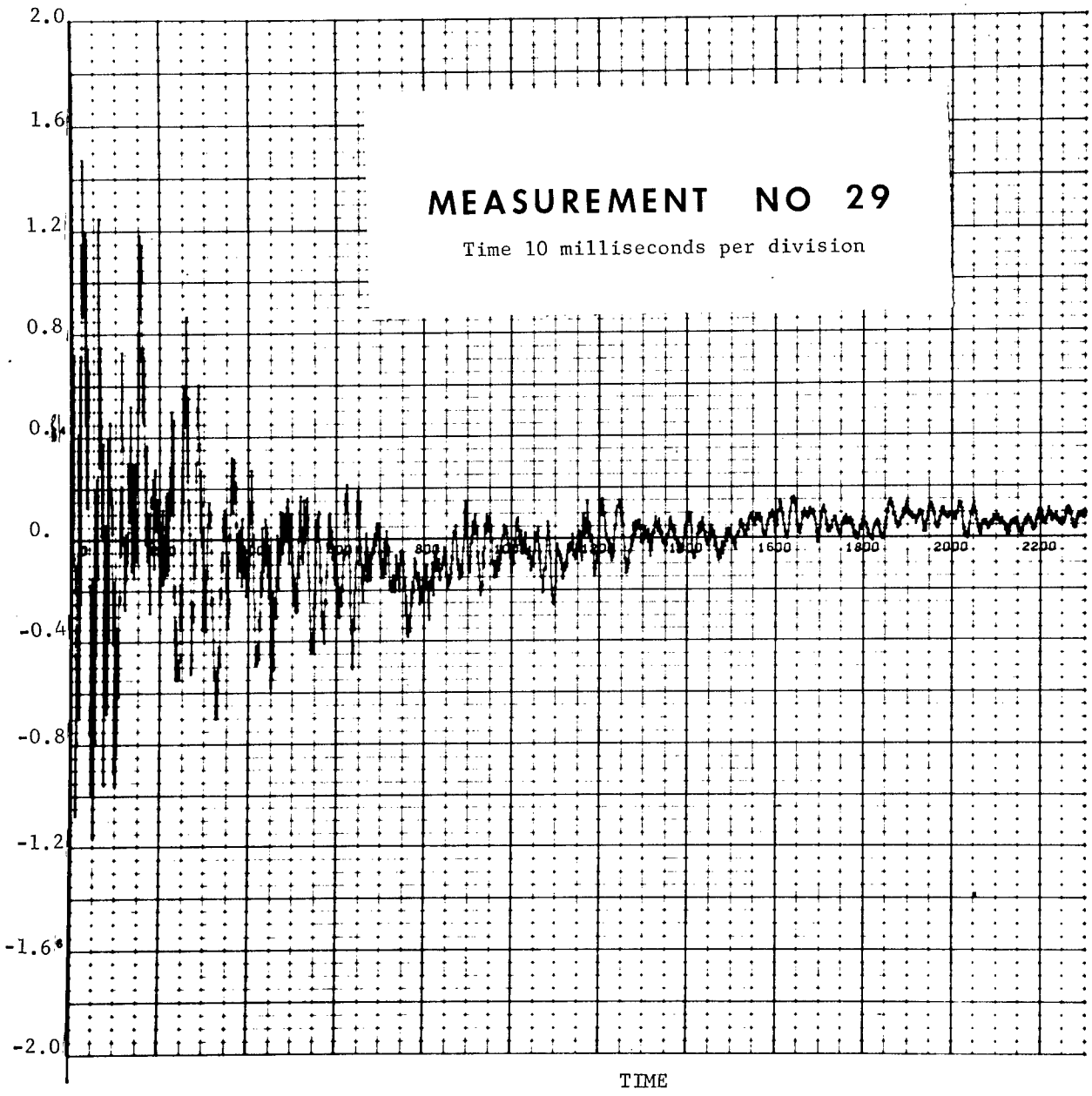

FIGURE 40. TEST DATA, OVERALL VIBRATION MEASUREMENT NO. 29

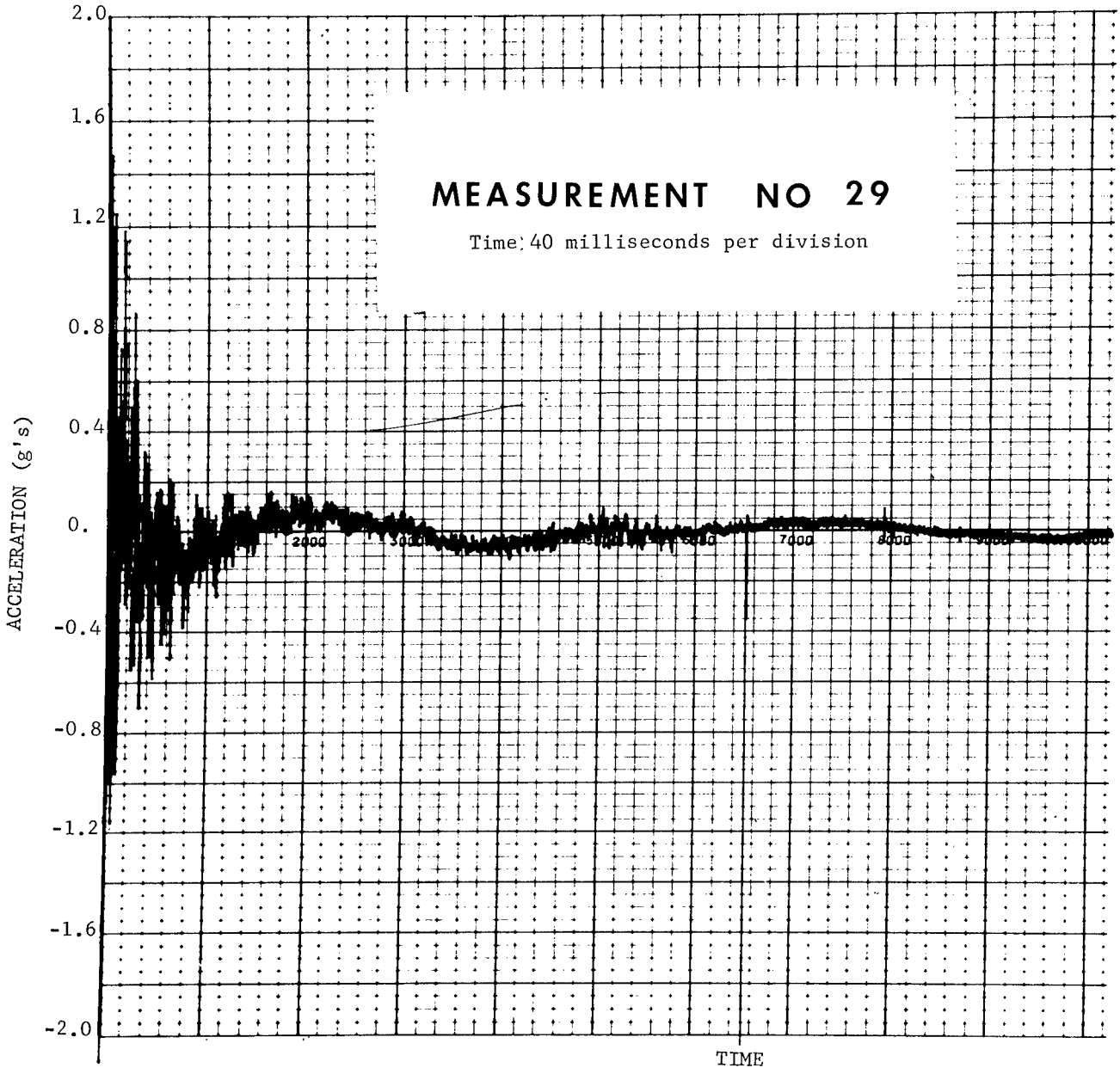

FIGURE 41. TEST DATA, OVERALL VIBRATION MEASUREMENT NO. 29

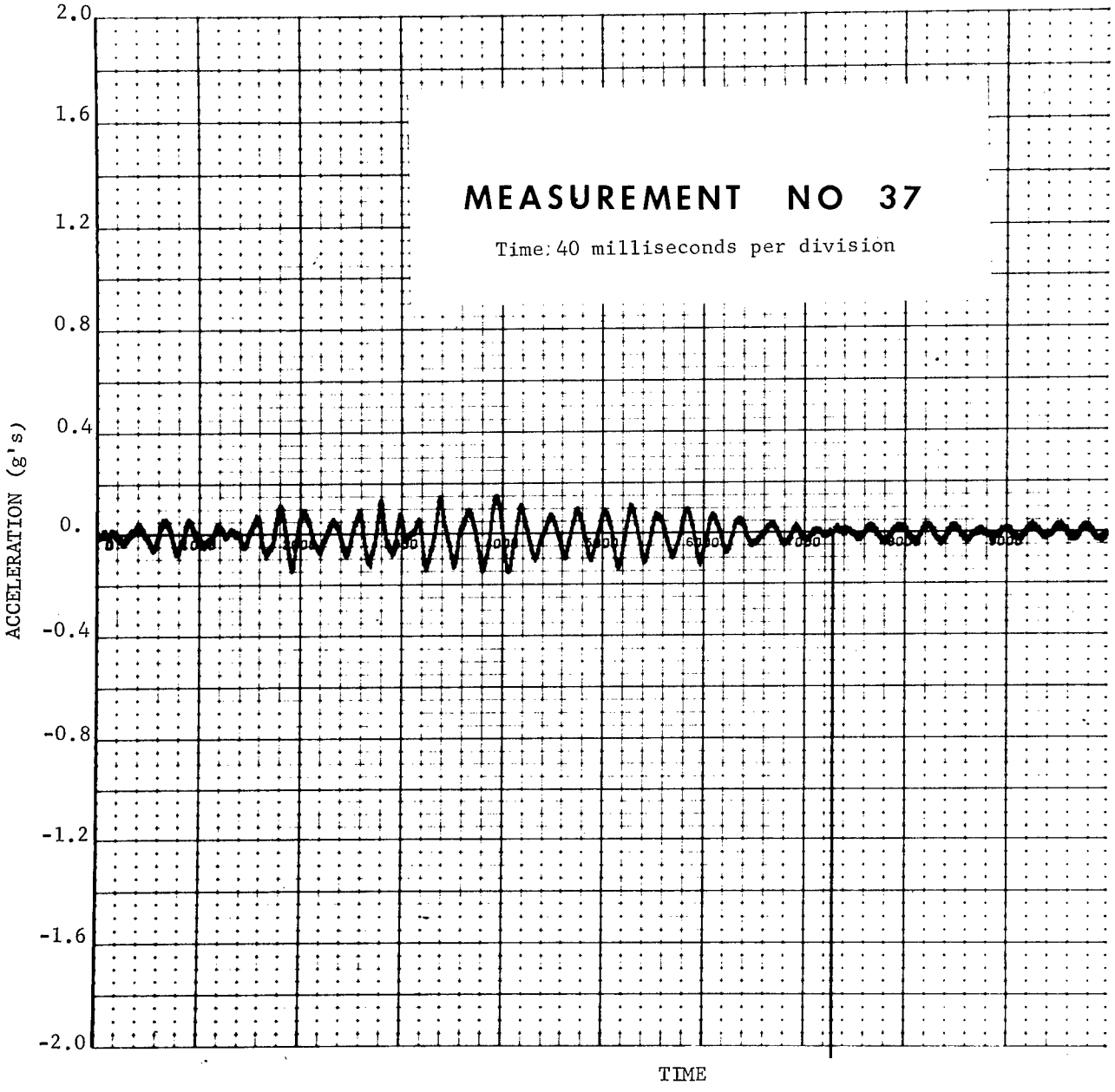

FIGURE 42. TEST DATA, OVERALL VIBRATION MEASUREMENT NO. 37

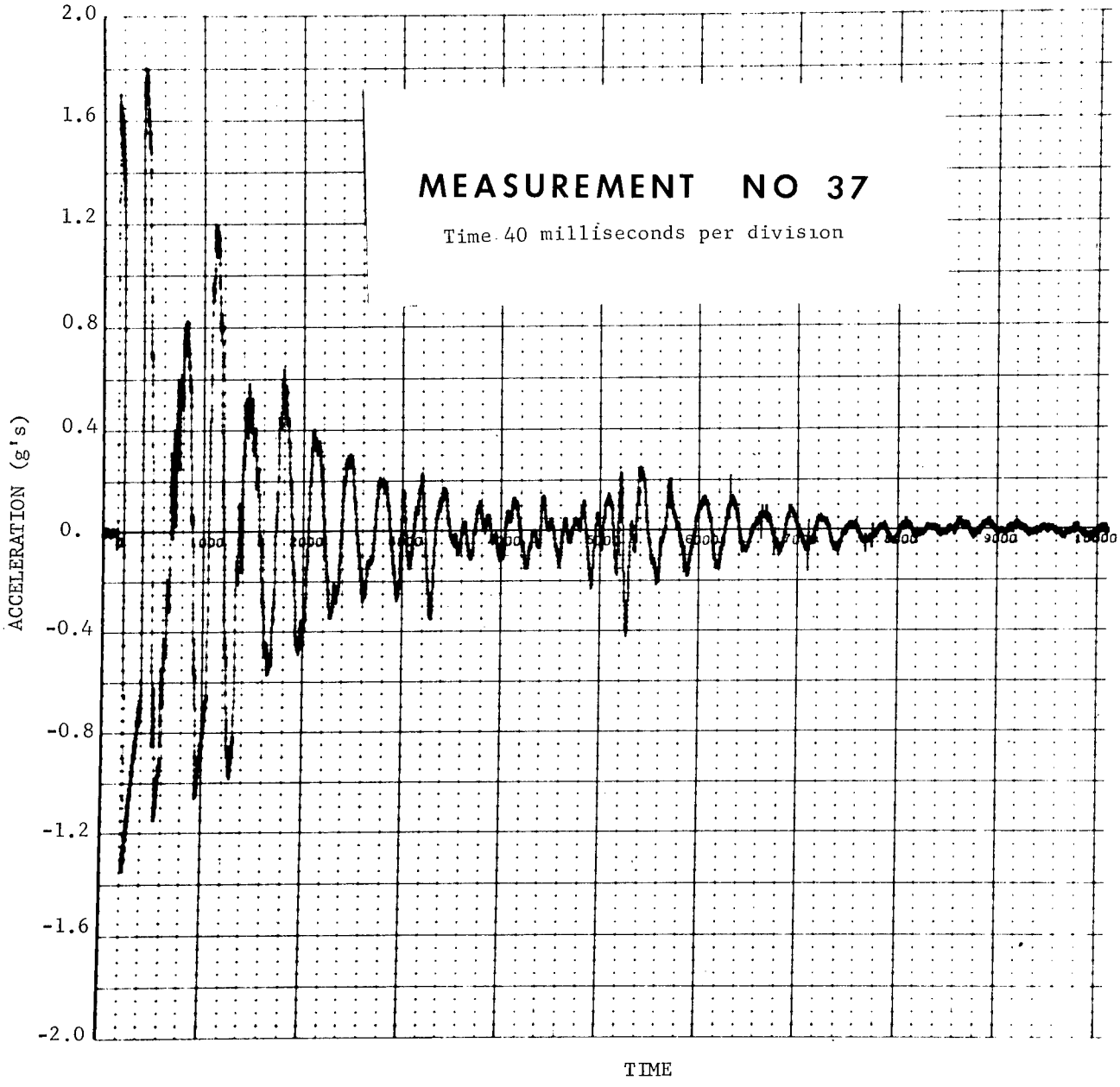

FIGURE 43. TEST DATA, OVERALL VIBRATION MEASUREMENT NO. 37

REFERENCES

1. Glasstone, Samuel: The Effects of Nuclear Weapons. DA Phamplet 39-3, United States Atomic Energy Commission, June 1957.

2. Anon.: Instrumentation for the Measurement of Air Blast and Ground Shock Intensities Generated by the Detonation of High Explosives. Explosives Research Group. Report Number DA-Q4-495-ORD674, July 13, 1956.

3. Hodgman, Charles D.: Handbook of Chemistry and Physics. Chemical Rubber Publishing Company, 1952.

4. Anon.: Technical and Administrative Arrangements for the 500 Ton TNT Trial. Suffield Experimental Station, Alberta, Canada, July 1964.

5. Anon.: Technical and Administrative Information for Operation Snowball. Suffield Experimental Station, Alberta, Canada, July 1964.

6. Robinson, Clark: Explosives, --Their Anatomy and Destructiveness, New York and London, 1944.

7. Republic Aviation Report RAC 1117-6, "First Annual Summary Report, Experimental Determination of System Parameters for Thin-Walled Cylinders," June, 1964.

"The aeronautical and space activities of the United States shall be conducted so as to contribute . . . to the expansion of human knowledge of phenomena in the atmosphere and space. The Administration shall provide for the widest practicable and appropriate dissemination of information concerning its activities and the results thereof."

—NATIONAL AERONAUTICS AND SPACE ACT OF 1958

NASA SCIENTIFIC AND TECHNICAL PUBLICATIONS

TECHNICAL REPORTS: Scientific and technical information considered important, complete, and a lasting contribution to existing knowledge.

TECHNICAL NOTES: Information less broad in scope but nevertheless of importance as a contribution to existing knowledge.

TECHNICAL MEMORANDUMS: Information receiving limited distribution because of preliminary data, security classification, or other reasons.

CONTRACTOR REPORTS: Technical information generated in connection with a NASA contract or grant and released under NASA auspices.

TECHNICAL TRANSLATIONS: Information published in a foreign language considered to merit NASA distribution in English.

TECHNICAL REPRINTS: Information derived from NASA activities and initially published in the form of journal articles.

SPECIAL PUBLICATIONS: Information derived from or of value to NASA activities but not necessarily reporting the results of individual NASA-programmed scientific efforts. Publications include conference proceedings, monographs, data compilations, handbooks, sourcebooks, and special bibliographies.

Details on the availability of these publications may be obtained from:

SCIENTIFIC AND TECHNICAL INFORMATION DIVISION

NATIONAL AERONAUTICS AND SPACE ADMINISTRATION

Washington, D.C. 20546